

ETD Archive

2012

Controlled Delivery of TGF- β 1 from PLGA Nanoparticles

Pratik K. Vaidya
Cleveland State University

Follow this and additional works at: <https://engagedscholarship.csuohio.edu/etdarchive>

 Part of the [Biomedical Engineering and Bioengineering Commons](#)

[How does access to this work benefit you? Let us know!](#)

Recommended Citation

Vaidya, Pratik K., "Controlled Delivery of TGF- β 1 from PLGA Nanoparticles" (2012). *ETD Archive*. 626.
<https://engagedscholarship.csuohio.edu/etdarchive/626>

This Thesis is brought to you for free and open access by EngagedScholarship@CSU. It has been accepted for inclusion in ETD Archive by an authorized administrator of EngagedScholarship@CSU. For more information, please contact library.es@csuohio.edu.

CONTROLLED DELIVERY OF TGF- β 1 FROM PLGA NANOPARTICLES

PRATIK VAIDYA

Bachelors of Engineering in Biotechnology

Shivaji University, Kolhapur, India

July 2009

submitted in partial fulfillment of requirements for the degree

MASTER OF SCIENCE IN BIOMEDICAL ENGINEERING

at the

CLEVELAND STATE UNIVERSITY

December 2012

This thesis has been approved
for the Department of Chemical and Biomedical Engineering
and the College of Graduate Studies by

Thesis Chairperson, Dr. Anand Ramamurthi
Department of Biomedical Engineering, Cleveland Clinic

Date

Dr. Joanne M. Belovich
Chemical and Biomedical Engineering Department, Cleveland State University

Date

Dr. Chandrasekhar Kothapalli
Chemical and Biomedical Engineering Department, Cleveland State University

Date

ACKNOWLEDGMENTS

I would begin with mentioning that I am grateful to Dr. Ramamurthi for giving me an opportunity to work under his lead, mentorship and guidance to develop an idea into a working project. Not only did he navigate me by providing insights, but also forgiving any mistakes made during this learning process. His patience and support, played a crucial role in shaping me for my future endeavors. Nonetheless, he will be looked up as a great source of inspiration by me, always.

My academic advisor, the departmental head of Biomedical Engineering department at Cleveland State University, Dr. Joanne Belovich, also a member on my master's thesis committee is gem of a person. I would like to thank her for laying a well-guided path from the day I got accepted at CSU till the end of my master's program. She encouraged me to adopt research and showed a great deal of support by recommending me to Dr. Ramamurthi.

I would next thank Dr. Chandrasekhar Kothapalli to agree to serve as a member of my master's thesis committee. His knowledge and thoughts have helped me in the courses I took under his supervision. Additionally, his past research in Dr. Ramamurthi's lab lays a foundation to my project today, and therefore, I consider myself fortunate enough to have him as an additional source of guidance.

I would like to convey special thanks to Dr. Balakrishnan Sivaraman, a post-doctoral fellow at Dr. Ramamurthi's lab at the Cleveland Clinic, without whom I couldn't have completed the project within 2 years. He is a senior colleague, a great mentor, and a good friend. He has spent countless hours training me and providing insights, and this surely accounts for every hurdle overcome that I faced during the course of this project.

Among my associates/colleagues at Dr Ramamurthi's lab, I would like to thank Dr. Chris Bashur for teaching and helping me with the complex procedures of RT-PCR. I would also like to thank Partha Deb for his patience and devotion of time with confocal imaging of my IF studies. Besides, I would like to thank every member of Ramamurthi lab who helped me in sailing through – Dr. Shyam Manisastry, Dennis Wilk, Dr. Lavanya Venkataraman, Ganesh Swaminathan, Sahithya Wintrich, Andrew Sylvester and Andrew Strong.

I would like to thank staff scientists, and personnel from other labs who engaged in cooperation and their help as and when needed. I would also like to thank Vinod Labhastewar Lab and its associates for their cooperation and letting us use their equipment. I would like to thank all core services at the Cleveland Clinic's Lerner research institute facility, especially imaging core for being there and eager to patiently train me on their equipment.

Last but never the least, I would like to thank my family and close friends for their love and support, and encouragement to move ahead in life. Especially, my parents Kiran and Pragna Vaidya; my younger brother, Parth are the most beloved people. It is next to impossible to be able to thank them in words. Their love, trust and support has clearly helped me being a better person.

CONTROLLED DELIVERY OF TGF- β 1 FROM PLGA NANOPARTICLES

PRATIK VAIDYA

ABSTRACT

Abdominal aortic aneurysms (AAAs) typically manifest as localized wall weakening and dilation of the infrarenal aorta, which grows gradually, and ultimately leads to fatal rupture. It is caused due to overexpression of proteolytic enzymes (matrix metalloproteases or MMPs) resulting into disruption of tissue structure, especially elastic matrix, which cannot be regenerated by adult vascular cells. On account of post-operative complications associated with their surgical repair, there is a critical need for developing non-surgical strategies for slowing and even regressing AAA growth. Recent studies in our laboratory have demonstrated that 1 ng/mL of transforming growth factor- β 1 (TGF- β 1) enhances regenerative repair by stimulating elastogenesis in healthy and aneurysmal rat aortic smooth muscle cell (SMC) cultures. The purpose of this study is to develop and characterize a nanoparticulate delivery system for localized, controlled and sustained delivery of TGF- β 1 to AAA tissue, for the elastogenic induction of SMCs. Accordingly, in this study, we have developed TGF- β 1 loaded poly (lactic-co-glycolic acid) PLGA nanoparticles using double-emulsion/solvent evaporation method. The NPs exhibited sustained release of TGF- β 1 over a period of at least 21 days in an in vitro aqueous system. The released TGF- β 1 from NPs inhibited the proliferation of mink lung epithelial cells, which confirmed the bio-functionality of TGF- β 1 protein post-encapsulation. Additionally, our IF studies demonstrated better fiber formation and orientation of elastin in TGF- β 1 NP treated cultures, which was potentially due to up-regulated expression of structural proteins like collagen and fibrillin-1 in TGF- β 1 treated cultures, as demonstrated by quantitative and qualitative

studies. Our studies also demonstrated up-regulated levels of lysyl oxidase (LOX), protein enzyme responsible for cross-linking elastin molecules into fibers in smooth muscle cell (SMC) extracellular matrix. However, quantitative analysis of insoluble and soluble elastin in TGF- β 1 NP treated cultures did not show its up-regulation, which is attributable to lower levels of TGF- β 1 (about 1/10th) released in aneurysmal rat SMC (EaRASMC) cultures, compared to our previously identified elastogenic doses. Nevertheless, this study carries high potential of clinical translation in future and could evolve as a method to regress AAAs versus current invasive methods.

TABLES OF CONTENTS

ABSTRACT	v
LIST OF TABLES	xii
LIST OF FIGURES	xiii
CHAPTER I	1
INTRODUCTION	1
1.1 Significance and current treatment of Abdominal Aortic Aneurysms (AAAs)	1
1.2 Matrix regenerative therapies	3
1.3 Localized, controlled delivery of elastogenic agents within AAAs	4
1.4 Project goals and specific aims	4
1.5 Organization of Thesis	5
CHAPTER II	6
BACKGROUND	6
2.1 Anatomy of blood vessel	6
2.1.1 Tunica intima	7
2.1.2. Tunica media.....	7
2.1.3. Tunica adventitia	8
2.2 Components of the vascular ECM	8
2.2.1 Collagen	8

2.2.2 Glycoproteins	9
2.2.3 Proteoglycans (PGs) and glycosaminoglycans (GAGs)	9
2.3 Elastin – Biological and structural roles	10
2.3.1 Biosynthesis of elastin and the elastic matrix assembly process	11
2.3.2 Malfunctions in the elastic matrix assembly process	13
2.3.3 Cellular interactions with tropoelastin	14
2.4 Proteolytic Disease: Abdominal Aortic Aneurysm (AAAs)	15
2.4.1 Etiology of AAAs	15
2.4.2 AAA pathology	16
2.4.3 Current strategies for diagnosis and treatment of AAAs	17
2.5 Elastin restorative strategies	20
2.5.1 Elastic matrix preservation strategies	21
2.5.2 Strategies for regenerative elastic matrix repair	23
2.5.3 Elastogenic Induction of SMCs	24
2.6 Elastogenic effects of TGF- β 1 in SMC cultures	25
2.7 Controlled, localized delivery of therapeutic biomolecules	28
2.7.1 Nanoparticles as delivery vehicles	28
2.7.2 Nanoparticle characteristics and implications to drug delivery	29
2.7.3 PLGA as NP matrices	30
2.7.4 Controlled delivery of TGF- β 1	31

CHAPTER III	33
MATERIALS AND METHODS	33
3.1 Development and characterization of TGF- β 1 loaded nanoparticles	33
3.1.1 Reconstitution of TGF- β 1	33
3.1.2 Formulation of nanoparticles	34
3.1.3 Efficiency of encapsulation of TGF- β in nanoparticles	35
3.1.4 Size and surface charge of TGF- β 1 nanoparticles	36
3.1.5 In vitro characterization of release of TGF- β 1 from nanoparticles	36
3.2 Determination of TGF- β 1 integrity in release media	37
3.3 Determination of functionality of released TGF- β 1	38
3.4 Cell Culture	39
3.4.1 Cell isolation methods	39
3.4.2 Determining in vitro cytotoxicity of TGF- β 1 loaded nanoparticles	40
3.4.3 Experimental design for culture studies for matrix assessment	40
3.5 Matrix Assays	42
3.5.1 DNA Assay	42
3.5.2 Fastin Assay	43
3.5.3 Hydroxy-Proline Assay	45
3.6 Immunofluorescence detection of elastic matrix assembly proteins	46
3.7 Western Blot for LOX.....	46

3.8 PCR	47
3.8.1 Isolation of mRNA	47
3.8.2 mRNA quantification.....	48
3.8.3 Reverse transcription of mRNA	48
3.8.4 PCR	49
CHAPTER IV	50
RESULTS AND DISCUSSION	50
4.1 Characterization of NPs	50
4.2 Release of TGF- β 1 from PLGA NPs	52
4.3 Bioavailability and Structural integrity of released TGF- β 1	55
4.4 Bioactivity of released TGF- β 1 in Mink Lung Cell cultures	56
4.5 Lack of cytotoxic effects of TGF- β 1 NPs on EaRASMCs	58
4.6 Effect of TGF- β 1 release from NPs on EaRASMC proliferation	59
4.7 Matrix Assays	61
4.7.1 Fastin Assay	61
4.7.2 Hydroxy-Proline Assay	62
4.8 Immunofluorescence detection of elastin, fibrillin-1 and LOX	64
4.9 Western Blotting for LOX	69

4.10 RT-PCR analysis for elastin and elastic matrix assembly proteins	71
CHAPTER V	73
CONCLUSIONS AND RECOMMENDATIONS	73
5.1 Conclusions	73
5.2 Future Recommendations	75
REFERENCES	77

LIST OF TABLES

Table 2.1 Biomolecular agents stimulating elastin synthesis and matrix deposition	25
Table 2.2 Biomolecular agents stimulating and also inhibiting elastin synthesis and deposition .	25
Table 2.3 Biomolecular agents inhibiting elastin synthesis and deposition	26
Table 2.4 An overview of advantages of bio-degradable PLGA NPs	28
Table 2.5 Different types of NP matrices and their applications	30
Table 3.1 Proteins associated with elastin synthesis and their primer sequences.....	49
Table 4.1 Data showing size, and surface charge (ζ - potential) and efficiencies of encapsulation of TGF- β 1 within the NPs, surface functionalized with PVA	51
Table 4.2 Data showing size, surface charge (ζ - potential) and efficiencies of encapsulation of TGF- β 1 within the NPs, surface functionalized with DMAB	52

LIST OF FIGURES

Figure 2.1 Schematic of Ultra Structure of a Blood Vessel.....	6
Figure 2.2 Structure of a GAG, hyaluronic Acid.....	10
Figure 2.3 Scanning electron microscopy (SEM) images showing possible elastic matrix superstructural forms	11
Figure 2.4 Elastic fiber assembly schematic.....	12
Figure 2.5 Schematic showing adverse effects by breakdown of elastic matrix on SMCs	15
Figure 2.6 Location of AAA in human anatomy	16
Figure 2.7 Current AAA repair strategies A) open AAA repair; B) Endovascular aneurysmal repair	20
Figure 4.1 Cumulative release of TGF- β 1 from NPs loaded with TGF- β 1 over 21 days, surface functionalized with DMAB.....	53
Figure 4.2 Cumulative release of TGF- β 1 from NPs loaded with TGF- β 1 over 21 days, surface functionalized with PVA.	54
Figure 4.3 Western blots of released TGF- β 1 (25 kDa)	55
Figure 4.4 Effect of TGF- β 1 and control treatment conditions on proliferation of MLCs.....	57
Figure 4.5 Results from LIVE/DEAD [®] assay	59
Figure 4.6 Results of DNA assay showing EaRASMCs count initially seeded and after 21 days of treatment with NPs loaded with TGF- β 1 and other control test conditions	60

Figure 4.7 Alkali-soluble and –insoluble elastic matrix deposition by EaRASMCs over 21 days of culture, as represented on a per cell basis.....	62
Figure 4.8 Collagen matrix deposition by EaRASMCs over 21 days of culture, using the OH-Pro assay and shown on a per cell basis	63
Figure 4.9 Representative images of controls and TGF- β 1 and/or NP-treated EaRASMC cultures IF-labeled for elastin (pink) at 21 days of exposure	66
Figure 4.10 Representative images of controls and TGF- β 1 and/or NP-treated EaRASMC cultures IF-labeled for fibrillin-1 (pink) at 21 days of exposure	67
Figure 4.11 Representative images of controls and TGF- β 1 and/or NP-treated EaRASMC cultures IF-labeled for LOX (pink) at 21 days of exposure	68
Figure 4.12 Western blot results for LOX (32 kDa - active protein, 28 kDa - cleaved LOX product).....	70
Figure 4.13 Quantification of LOX-protein band intensities, normalized to band intensities of β -actin as visualized in western blots	70
Figure 4.14 Gene expression of proteins of interest represented as RFU from TGF- β 1 NP treated and untreated cultures	72

CHAPTER I

INTRODUCTION

1.1 Significance and current treatment of Abdominal Aortic Aneurysms (AAAs)

Aortic aneurysms (AAs) represent localized wall weakening and dilation of the aorta due to disruption of tissue structure, typically secondary to trauma, infection, atherosclerosis, vascular hypertension, and overexpression of proteolytic enzymes [1]. If untreated, AAAs can gradually distend to fatal rupture [2]. Depending on their incidence on the aorta, AAs are classified as abdominal aortic aneurysms (AAAs), thoraco-abdominal aortic aneurysms, or thoracic aortic aneurysms (TAAs). AAAs occur in the region between the renal and iliac bifurcations of the aorta, are typically asymptomatic, and are often detected only when ultrasound or MRIs are presumptively performed to screen for the condition [3]. The condition is most common in senior males (>70) in the United States and causes up to 15,000 deaths per year [4]. Studies have shown that there is low prevalence of AAAs in women compared to men, but women with smoking history and/or heart disease are at equally high risk of AAA occurrence [5].

AAAs are caused due to the fragmentation of elastin and elastic fibers by proteolytic enzymes called matrix metalloproteinases (MMPs), which are released by inflammatory cells infiltrating the AAA site following an initial injury or stimulus (e.g., smoking, vasculitis, chronic hypertension etc) [1, 6, 7]. Currently, open surgical repair and endovascular aneurysmal repair (EVAR) are surgical, and the only means of AAA repair [8]. Open repair is highly invasive, and involves abdominal laparotomy, followed by surgical removal of the dilated aorta and its replacement with Teflon graft [9]. EVAR is a minimally-invasive procedure involving percutaneous access to the affected area and placement of a stent graft to flow-exclude the AAA region and prevent further dilatation [10]. High mortality rate due to surgical complications, graft issues pertaining to lack of biocompatibility, occurrence of endoleaks, and migrating stent grafts, and inability of aged individuals to withstand surgical procedures can be problematic and frequently entail the need for surgical re-intervention [11]. Considering these limitations of surgical AAA repair, there is a critical necessity for novel, non-surgical methods to treat and potentially prevent AAAs.

Currently there are no non-surgical means to treat AAAs. Considering the fact that the disruption or loss of elastin and elastic matrix is a critical component of AAA progression, its repair and/or regeneration offers a promising modality for potentially stabilizing or even regressing AAA growth. However, the process of elastin synthesis and matrix assembly is highly complex, and is particularly limited in adult tissues by the inherent deficiency of adult vascular smooth muscle cells (SMCs) in synthesizing elastin and assembling it into matrix superstructures (e.g., fibers and fibrous sheets). Additionally, the disruption of elastin/elastic fibers by proteolytic enzymes (MMPs) overexpressed at sites of vascular tissue injury or

disease/inflammation are also hurdles to efficient regeneration of elastic matrix, and their net accumulation via this process.

Recently, strategies to preserve and stabilize existing elastic matrix within AAAs have been investigated, which involve suppression of MMP over-production and over-activity within AAAs. These have included delivery of pharmacological agents (e.g., doxycycline or DOX) [12, 13], tissue inhibitors of matrix metalloproteinases (TIMPs) [14], and the inhibition of transcription factors mediating mRNA expression for MMPs [15]. Nevertheless, these strategies have been limited by their potential ability to only slow AAA growth, or at best, not demonstrated to date, arrest AAA growth, but not regress the AAA towards a healthy state. To achieve the latter, active regenerative repair of elastic matrix and net new elastic matrix accumulation is mandated.

1.2 Matrix regenerative therapies

Approaches pertinent to tissue engineering and its *in vivo* counterpart, regenerative medicine approaches, have gained popularity in combining cells, biomolecules, scaffolds and dynamic culture approaches to regenerate or restore the function of diseased or structurally-disrupted tissues. Prior studies have identified various biomolecules that stimulate the process of cellular elastic matrix assembly *in vitro*. For example, our laboratory has shown the elastogenic effects of transforming growth factor β 1 (TGF- β 1) [16], insulin-like growth factor-1 (IGF-1) [17] and hyaluronan oligomers (HA-o) [16, 17] in healthy [17] and aneurysmal SMC cultures [16, 17]. One way TGF- β 1 is hypothesized to enhance elastic matrix regeneration is by up-regulating lysyl oxidase (LOX) mRNA expression and protein synthesis, leading to increased crosslinking of elastin precursor molecules towards enhancing elastic fiber assembly [18]. TGF- β 1 also is

known to down-regulate MMP-2 and -9 mRNA expression /protein synthesis in a dose specific manner [18, 19]. Our lab previously showed 1.0 ng/mL of TGF- β 1 dose to significantly up-regulate elastin matrix synthesis by vascular SMCs (rat and human) [16, 17].

1.3 Localized, controlled delivery of elastogenic agents within AAAs

While TGF- β 1 has pro-elastogenic effects, it is important to note that excessively high TGF- β 1 doses or their systemic delivery *in vivo* could have adverse effects. For example, it has been shown that at very high doses, TGF- β 1 causes osteogenic differentiation of SMCs and enhances matrix calcification [16, 20]. Also TGF- β 1 over expression which has shown to stabilize AAAs [21], is known to initiate TAAs [22], common in Marfan syndrome patients [22, 23]. Therefore for *in vivo* AAA therapy, it is essential to ensure a localized, controlled and sustained delivery of therapeutic agents such as TGF- β 1 via suitable carrier. This thesis project is focused on the design and development of polymeric nanoparticles (NPs) using poly (lactide-co-glycolide) (PLGA) for the encapsulation and localized and controlled/predictable delivery of TGF- β 1 to AAAs in enhancing elastin synthesis. In this study, we evaluate efficacy of these NPs and the ability of the released agent to influence elastic matrix deposition *in vitro* aneurysmal SMC cultures.

1.4 Project goals and specific aims

As discussed in previous sections, this project seeks to achieve elastogenic induction of aneurysmal rat aortic smooth muscle cells (EaRASMCs) in 2-dimensional (2-D) cultures, via controlled, sustained delivery of TGF- β 1 from PLGA nanoparticles. More specifically, we aim to:

- **Specific Aim 1:** Design and formulate PLGA NPs encapsulating TGF- β 1 and determine their release characteristics as a function of TGF- β 1 loading.
- **Specific Aim 2:** Evaluate functional effects of TGF- β 1 released from NPs on elastic matrix deposition in 2-D cultures of EaRASMCs.

1.5 Organization of Thesis

Chapter 2 presents detailed background information on the extracellular matrix (ECM) components of blood vessels, the structural and biological roles of elastin, and the process of its synthesis and assembly into a matrix. The chapter further discusses AAAs patho-physiology towards understanding the critical role played by the loss/degradation of elastin in AAA progression. Finally, the rationale for the use of, and basis for the development and design of polymeric nanoparticles for localized, controlled, and long-term delivery of elastogenic factors for elastogenic induction of SMCs, is elucidated.

Chapter 3 describes the materials and methods employed in fabricating PLGA nanoparticles encapsulating TGF- β 1, the experimental design, and details on specific assays performed to characterize NPs, their release of TGF- β 1, to evaluate TGF- β 1 bioavailability and bioactivity, as well as its *in vitro* elastogenic effects in 2D cell culture systems.

The results from these assays are discussed in **Chapter 4**, providing critical insights into the optimization of TGF- β 1 encapsulation and release, and its subsequent effects on enabling the elastogenic induction of aneurysmal SMCs *in vitro*.

Finally, **Chapter 5** provides perspectives on the results obtained and suggest possible directions in which the research can be focused, towards developing targeted AAA therapies.

CHAPTER II

BACKGROUND

2.1 Anatomy of blood vessel

The vascular wall is composed of three concentric layers proceeding outwards from the lumen; these are the *tunica intima*, *tunica media* and *tunica adventitia*. These layers play critical roles in determining the structure and function of blood vessels, and contain characteristic cell types and extra cellular matrix (ECM).

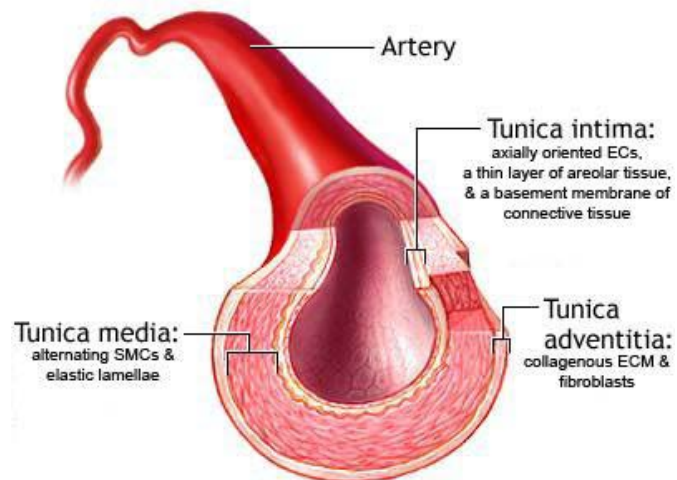


Figure 2.1 Schematic of Ultra Structure of a Blood Vessel [24]

2.1.1 *Tunica intima*

The *tunica intima* forms the innermost layer of a blood vessel, which is directly in contact with blood flow. It consists of axially-oriented endothelial cells (ECs) and a basement membrane which is typically composed of loose connective tissue. The basement membrane is comprised of type IV collagen, laminin, entactin and proteoglycans (heparan sulfate) [25, 26] and adjoins the internal elastic lamina [26]. The basal lamina acts as a molecular barrier between the endothelial layer and the underlying mass of connective tissue. The ECs are an integral part of the vessel wall, playing a critical role in attenuating thrombosis, modulating angiogenesis, and regulating blood pressure by signaling underlying smooth muscle cells (SMCs), by release of endothelium derived relaxing factor (EDRF) now identified as nitric oxide (NO) [27]. In addition, the ECs serve as a barrier to prevent/limit free diffusion of cells and blood fluids/proteins [28]. They also influence cell polarity, proliferation and differentiation by binding various growth factors (GFs) and regulate cell metabolism [28, 29].

2.1.2 *Tunica media*

As the name suggests, this layer is the middle layer of the vascular wall, and in large elastic vessels (e.g., aorta) is bound on the intimal side by the internal elastic lamina, and on the adventitial side by the external elastic lamina. The *tunica media* is predominantly composed of SMCs and sheets composed of closely enmeshed elastic fibers arranged in concentric alternating bundles (lamellae) [30]. The SMCs are responsible for the synthesis of elastin molecules that compose elastic fibers, which then assemble/organize into lamellae. The type and function of the blood vessel determines the number of elastic lamellae; for example, conduction arteries like the aorta possess 40-70 lamellar layers whereas peripheral and other arteries are known to contain 3-

40 layers [31]. The elastic lamellae are surrounded by sheaths of collagen I, III, V fibers. On account of the significant amount of elastin fibers and elastic matrix present in this layer, this layer plays a critical role in the recoil of blood vessels following stretch imposed by flow of blood pumped out by the heart during cardiac systole.

2.1.3 *Tunica adventitia*

The *tunica adventitia* is the outermost layer of the vessel and consists of a collagenous ECM, terminal nerve fibers, and surrounding connective tissue containing fibroblasts [32]. This fibrous, collagen-rich layer (mostly collagen types I and III in aortae) prevents vessel over expansion due to stretch imposed by high luminal blood pressure [33]. Additionally, the adventitia helps innervate the SMCs in the *tunica media*, supplies blood to the vessel tissue itself through a network of capillaries called *vasa vasora*, so as to maintain cell viability within, and also to protect the blood vessel from surrounding tissues [34].

2.2 Components of the vascular ECM

2.2.1 *Collagen*

Collagen is a structural protein abundantly found in blood vessels, comprising approximately 70% by dry weight in the aorta [35]. Collagen fibers are primarily responsible for providing support and tensile strength to the vessel [36]. At the molecular level, collagen has a triple helix of two identical $\alpha 1$ -polypeptide chains, with a slightly different $\alpha 2$ chain, and has an amino acid composition that predominantly contains glycine, proline and hydroxyproline. Collagen types I, III and V participate in fiber formation. Types I and III are the predominant types of collagen found in vasculature [37]. Type V collagen is associated with types I and III

and serves to regulate collagen fiber formation and connect the basement membrane to the underlying ECM [37]. In addition to its structural role, collagen is also involved in promoting cell differentiation and attachment [38], and further serves to modulate SMC phenotype, promoting a more contractile, quiescent phenotype.

2.2.2 Glycoproteins

Fibronectin and laminin are glycoproteins (i.e., biomolecules composed of proteins and carbohydrates) that are vital to vascular homeostasis, but are not as abundant as collagen in the matrix. Unlike collagen, they do not perform structural roles but serve to interact with cells via integrin receptors to modulate their behavior, and also facilitate their interaction with other major ECM components [39]. Fibronectin is a high molecular weight glycoprotein (~440kDa) that binds to receptor proteins spanning the cell membrane (integrins) and to the ECM. It can also specifically bind to other molecules such as collagen and fibrin. It has an important role in matrix deposition [40] and coagulation [41], as well as in the activation and migration of inflammatory cells [42]. Laminin is a major protein found in the basal lamina and is associated with type IV collagen networks. It binds to cell membranes through integrins and other plasma membrane molecules to contribute to cell attachment, differentiation, cell phenotype and movement [43, 44]. Thus, glycoproteins play an important role in ECM formation and deposition and various cell processes.

2.2.3 Proteoglycans (PGs) and glycosaminoglycans (GAGs)

PGs and GAGs constitute the amorphous ground substance surrounding vascular cells. PGs are complex macromolecules that contain a core protein covalently bound to at least one

GAG chain. They are functionally associated with collagen and elastic fibers in the ECM [45], binding cations and water due to their anionic groups, and regulating the movement of molecules through the matrix assembly. GAGs (such as hyaluronan, chondroitin sulfate, dermatan sulfate and keratan sulfate) are long unbranched polysaccharides consisting of a repeating disaccharide unit (see **Figure 2.2**). This repeat unit consists of a hexose (six-carbon sugar) or hexuronic acid bound to a hexosamine. The availability of sulfate groups and carboxylate groups on their uronic acids residues imparts an overall negative charge to the molecules themselves. These polysaccharides bind water to become highly hydrated gel-like structures that resist compressive forces while permitting rapid diffusion of nutrients, metabolites, and hormones between blood and tissue [45] .

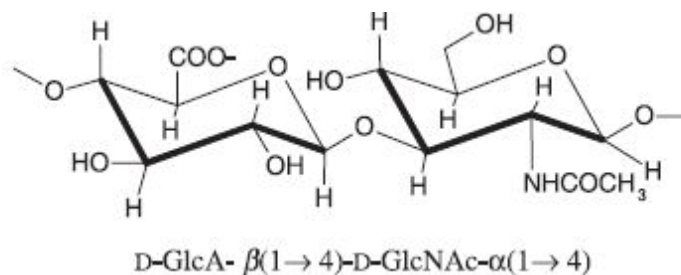


Figure 2.2 Structure of a GAG, hyaluronic Acid [46]

2.3 Elastin – Biological and structural roles

Elastin is a major structural protein in the ECM of elastic tissues such as large blood vessels, vocal folds, skin, vaginal wall, lungs and bladder. It is primarily synthesized by SMCs [47], as well as fibroblasts [48]. In the aorta, elastin contributes to about 50% of tissue dry weight [49]. In the *tunica media*, elastin protein is incorporated into and organized as fibers and sheets (lamellae) which are circumferentially arranged, forming alternating layers with SMCs [30]. The general organization of elastin in the ultrastructure of blood vessels could either be

singular or networked mesh-like fibers or non-fibrillar matrix structures like sheets [50], as shown in **Figure 2.3**.

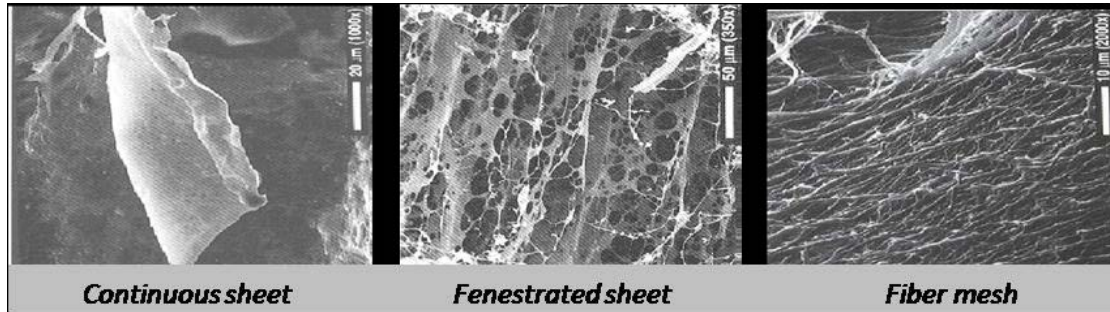


Figure 2.3 Scanning electron microscopy (SEM) images showing possible elastic matrix superstructural forms [50]

2.3.1 Biosynthesis of elastin and the elastic matrix assembly process

The process of elastic matrix assembly is highly complex, and occurs primarily during fetal development, and the neonatal stage [51]. In most tissues, with certain exceptions (e.g., skin) the process of matrix assembly and maturation shows slow down following adolescence. In brief, elastin is synthesized by SMCs in the vessel wall as a precursor molecule (tropoelastin; MW = 72 kDa), a hydrophobic protein containing a highly conserved amino acid sequence (Val-Gly-Val-Ala-Pro-Gly), rich in glycine (33%) and proline (10%). In addition, the protein contains amino acids such as hydroxyproline (1%), and alanine, valine and leucine (collectively 40-50%) [52]. The elastin binding protein (EBP) present on the outer plasma membrane of SMCs binds to tropoelastin, extruded from the intracellular space, and protects it from degradation [53, 54], while prompting their nucleation and cross-linking. Subsequently, the nuclei interact with a microfibrillar network of glycoproteins, when the nuclei of tropoelastin molecules dissociate from their complex with the EBP. These microfibrils, of which fibrillin-1 forms the major component, are highly aligned and play a crucial role in the coalescence of tropoelastin nuclei to

form amorphous elastin deposits [55]. In particular, fibulin-4 and fibulin-5 have been demonstrated to mediate tropoelastin interactions with the microfibril network [56]. The role of fibulin-2 in the elastic matrix assembly process, however, is less clear, as one study has suggested that it works co-operatively with fibulin-5 [57], while another study ruled out its role in the process [56]. Adjacent elastin molecules are then further cross-linked by a copper dependent enzyme lysyl oxidase (LOX) and the deposits gradually extended to form mature elastin fibers [58].

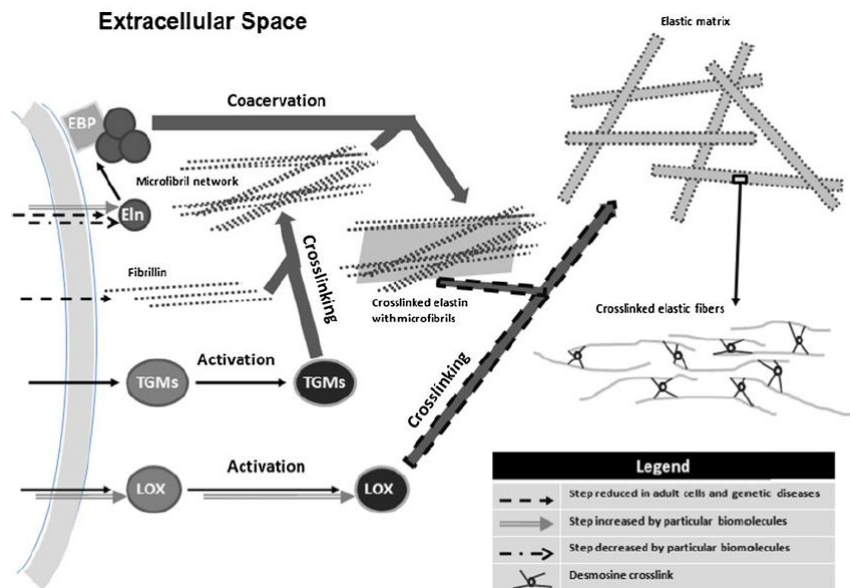


Figure 2.4 Elastic fiber assembly schematic [59]

LOX deaminates lysines in tropoelastin molecules, which then become covalently bound via desmosine and isodesmosine crosslinks to form the elastic fibers. The mature elastin fibers thus consist of a central core of cross-linked elastin surrounded by a network of aligned microfibrils containing fibrillin-1 as a major component [60, 61]. These fibers typically range in diameter from 300 nm to greater than 1 μm [60, 61]. The elastin fibers along with the highly aligned microfibrillar scaffold play a critical role in the mechanics and function of the tissue, and

impairment in either of these components or in any of the matrix assembly steps may lead to changes in tissue function and mechanics.

2.3.2 Malfunctions in the elastic matrix assembly process

On account of the complexity of elastogenesis mentioned above and the poor elastogenic capacity by adult cell types, the generation and/or regeneration of elastin and elastic matrix structures by healthy or diseased SMCs is problematic in vascular context, the primary challenge as mentioned, lies in inherently poor elastogenicity of adult vascular SMCs due to continuous decrease in expression of elastin producing mRNA [62, 63]. In addition, poor cellular ability to recruit and cross-link elastin precursors into elastic fibers/matrix, are major hurdles to assembly of elastic matrices. The over-expression of proteolytic enzymes by diseased/activated SMCs and inflammatory cells recruited to diseased/injured tissue sites also cause significant matrix disruption [64]. Collectively, these two processes are primarily responsible for the inability of cells in adult tissues to achieve net accumulation of mature, cross-linked and structurally appropriate elastic matrix, especially since elastin synthesis and assembly is insufficient relative to its degradation.

In addition to inherent deficiencies in elastogenesis, related to the aging process, syndromic disorders can further compromise elastin synthesis and matrix assembly. For example, genetic disorders such as Marfan syndrome involve mutation of a gene that encodes for fibrillin-1 which is major component of microfibrils having a role in elastin fiber formation [65]. As a result, poor or lack of deposition of elastin matrix, early fragmentation of elastic fibers and/or accumulation of amorphous elastin occurs in the *tunica media* of aortic walls. Patients with William-Beuren syndrome (WBS) suffer from arterial stenosis and hypertension (leading

into AAA) as a result of a deleted allele in elastin (ELN) forming gene. As a result of this, production of tropoelastin is affected which leads to incomplete formation of elastic fibers altogether, and far fewer elastic lamellae within the aortic wall [66]

2.3.3 Cellular interactions with tropoelastin

In addition to being incorporated into elastic fibers, tropoelastin influences chemotaxis [67] and adhesion [68] of fibroblasts, while also being shown to stimulate vasodilation and regulate intracellular Ca^{2+} in vascular ECs and SMCs [69]. These cellular responses are suspected to elicit feedback control during elastogenesis [70]. Mature elastin has numerous effects on vascular SMCs including inducing actin stress fiber orientation, inhibiting SMC proliferation and regulating cell migration, and maintaining SMCs in a healthy quiescent phenotype [71]. It has been proposed that in vascular SMCs, elastin activates a G-protein coupled pathway that further downstream inhibits adenylate cyclase and reduces cAMP (inhibitor of elastin synthesis) levels [72].

SMC interactions with intact elastin also mediate their survival, phenotype, proliferation, migration and differentiation [73]. For example, SMCs switch from contractile phenotype to a more synthetic phenotype under pathologic conditions wherein elastin tends to get fragmented [74, 75]. It has been shown that native elastin promotes hyperproliferation of vascular SMCs and also controls their differentiation [73]. Studies have shown that elastin controls the proliferation rate of SMCs and its aggressive migration in response to chemoattractants [74, 76].

As mentioned earlier, under pathologic conditions, elastin is broken down by enzymes to generate elastin peptides at an accelerated rate, which upregulate SMC proliferation and activation of phagocytic cells [70]. These elastin peptides interact with cells (e.g., SMCs,

macrophages) to elicit biological effects such as matrix metalloproteinase (MMP) overexpression, greater Ca^{2+} influx, enhanced vasorelaxation and chemotactic activity [74], which can then lead to undesirable outcomes such as vascular calcification, and enhanced matrix proteolysis.

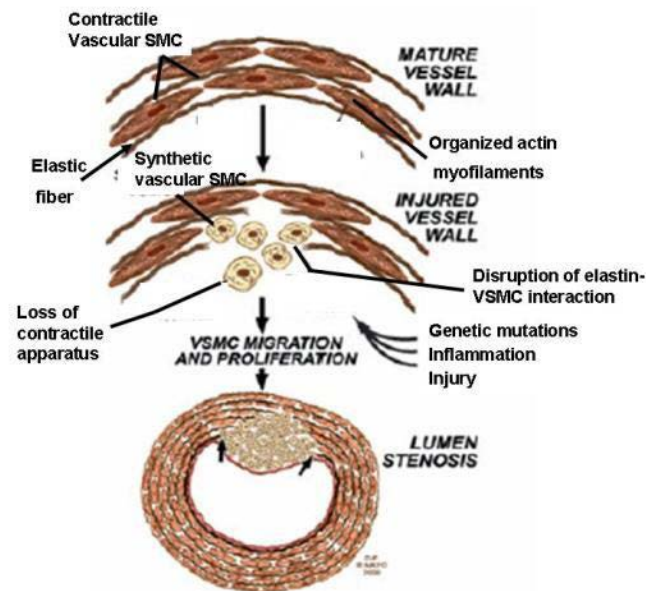


Figure 2.5 Schematic showing adverse effects by breakdown of elastic matrix on SMCs [74]

2.4 Proteolytic Disease: Abdominal Aortic Aneurysm (AAAs)

2.4.1 Etiology of AAAs

Aortic aneurysms are progressive, localized expansions of the aorta caused by pathological weakening of the vessel wall that may have final outcomes of dissections (tears) and fatal rupture. Abdominal aortic aneurysms (AAAs) occur in the descending aorta below diaphragm between the infra-renal and iliac bifurcations. The primary risk factors for AAA development are smoking, atherosclerosis, chronic hypertension, and certain inherited AAAs can

also occur secondary to vascular infection and inflammation (vasculitis) or abdominal trauma [1, 6, 7, 77]. The fatality rate for this condition is approximately 15,000 deaths per year [4]

In particular, elderly Caucasian men have been identified to represent a high risk population for AAA development, with incidence in nearly 2-6% of individuals in this demographic [78].

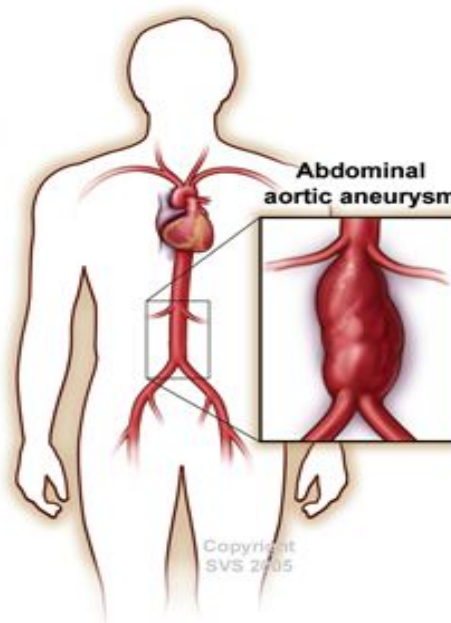


Figure 2.6 Location of AAA in human anatomy (Adapted from <http://www.vascularweb.org/vascularhealth/pages/abdominal-aortic-aneurysm.aspx>)

2.4.2 AAA pathology

AAA development is associated with the infiltration of inflammatory cells, such as macrophages and lymphocytes, and is often observed in concurrence with the deposition of atherosclerotic plaques in the aortic wall [79]. In an attempt to remodel the tissue and eliminate diseased cells, the inflammatory cells chronically overexpress cytokines that trigger release of matrix degrading metalloproteases (MMPs). The chronic enzymatic degradation of elastic matrix in the vessel wall that results due to the overexpression of elastinolytic MMP-2 and -9 by the

infiltrating inflammatory cells leads to slow AAA growth. Thus, the initial AAA development stage is characterized by a reduction in the quality and quantity of elastic fibers, accumulation of proteoglycans, and loss of SMCs [80]. The ECM in and around the AAA site varies due to numerous parameters including initiating cause, size and location, proximity to site of injury, stage in development, inflammatory cell involvement and presence of a thrombus [81, 82]. For instance, the AAA site exhibits significant loss of both elastin and collagen. On the other hand, sites distal and proximal to it exhibit rapid loss of elastin with minimal net collagen loss, which can be attributed to the differential hemodynamic load the vessel experiences in these two regions [83]. Regardless, it is salient to note that disrupted collagen undergoes replacement via regeneration, which occurs as a compensatory response to increased wall stress perceived by SMCs upon wall thinning. On the other hand, the elastic matrix does not show such recovery, due to poor elastogenicity of adult SMCs.

2.4.3 Current strategies for diagnosis and treatment of AAAs

AAAs are typically asymptomatic, rendering their detection difficult. However recognizing high risk factors for AAAs, pro-active ultrasound screening is now approved for high risk senior men. Most of such detected AAAs (> 90%) tend to be small (diameter less than 5.5 cm) [84]. The AAAs grow gradually (~10% per year) [85] over five-years or more until they reach a critical size (> 5.5 cm maximal diameter), at which point they become prone to rupture. During this period, they are passively monitored via ultrasound. At the critical stage, removal of the aneurysmal region of the aorta by open surgical means is recommended, or the diseased segment is replaced with a synthetic vascular graft. Grafts used for AAA repair may be autologous, allogeneic, xenogeneic, or synthetic, depending on their application. Characteristics

of an ideal graft include mechanical strength, compliance, kink resistance, non-immunogenicity, low thrombogenicity, among other properties [86].

Although autologous grafts (e.g., greater saphenous vein or internal mammary artery) [87] are the most viable clinical option for bypassing of diseased blood vessels, on account of their lack of immunogenicity, they are often limited by a lack of quality and availability. In the case of AAAs, these small vessels are also mismatched size-wise with the aorta. Allogeneic grafts are an attractive substitute due to identical structure, mechanical properties and size-matches and are retrieved from vessels from deceased fetuses, and cadavers [88]. However, allogeneic tissues may elicit an immune response from the recipient and graft rejection may occur, which would require lifelong immuno-suppressive therapy to ensure allograft survival [89].

Xenogeneic (e.g., bovine or porcine) materials, on the other hand, could lead to problems of end-stage organ failure, and disease transmission [90]. Although xenografts can be processed (e.g., SDS treatment) to avoid the immune response, this process could compromise the structural integrity of the resulting acellular matrix composed of elastin and collagen, leading to compliance mismatch, elastin degradation, inducing thrombogenicity and mechanical stiffening [90]. Autologous vascular cell seeding of the luminal surface establishing a confluent monolayer of cells can be used to alleviate the above problems to certain extent [91].

As an alternative to human- or animal-derived grafts, synthetic polymer grafts are usually used in blood vessel replacement. Most popular kinds of polymeric grafts available are Dacron, Teflon and polyurethanes [92]. Dacron and Teflon have shown to have greater tensile strengths and non-biodegradability. However, compliance-related issues and formation of neointima compromise the usability of synthetic grafts [92]. Polyurethane grafts on the other hand, have an

added advantage of suitable porosity and the ability to regulate compliance. The major disadvantage of polyurethane grafts is their very slow degradation with time [93].

Open AAA repair is the traditional method for surgical repair/treatment of aneurysms for the majority of patients. Briefly, this method involves laparotomy and complete removal of the dilated aorta [8]. This portion is replaced by a Teflon graft which is observed to have a durability of 20-30 years. However, the mortality rate during the first 30 days can be as high as 4-12% due to postoperative side effects such as myocardial infarction, renal failure, paraplegia, hepatic dysfunction and acute respiratory distress syndrome [8, 94].

Considering the risks due to the invasive procedure and high mortality rates, a relatively less invasive method called endovascular aneurysm repair (EVAR) was introduced in 1990's. It involves access to the affected aorta through femoral arteries percutaneously as opposed to large incisions made in open repair. An endovascular stent graft is inserted and guided to the aneurysm site using a catheter. The strategically placed stent graft permits blood flow and avoids AAA growth due to hemodynamic forces on aortic wall in and around the former site of the AAA. However, limited anatomical (e.g., size, age) suitability, endoleaks due to graft failure/movement and lifelong surveillance are the disadvantages of EVAR [8]. Currently, unavailability non-surgical procedure during the 5 year surveillance period for growing aneurysms and population unable to endure surgeries are major hurdles in longevity of aneurysmal patients.

As elucidated from previous sections, there are currently no pharmacological therapies available for AAA that can prevent its growth to rupture. These pharmacological therapies can be a blessing, especially for elderly patients who cannot withstand/survive the surgeries and/or inefficacies due to complications of surgeries like EVAR. Therefore, based on the inherent

limitations/disadvantages of surgical and interventional AAA repair, there is a critical need for designing and developing non-surgical modalities to treat AAAs.

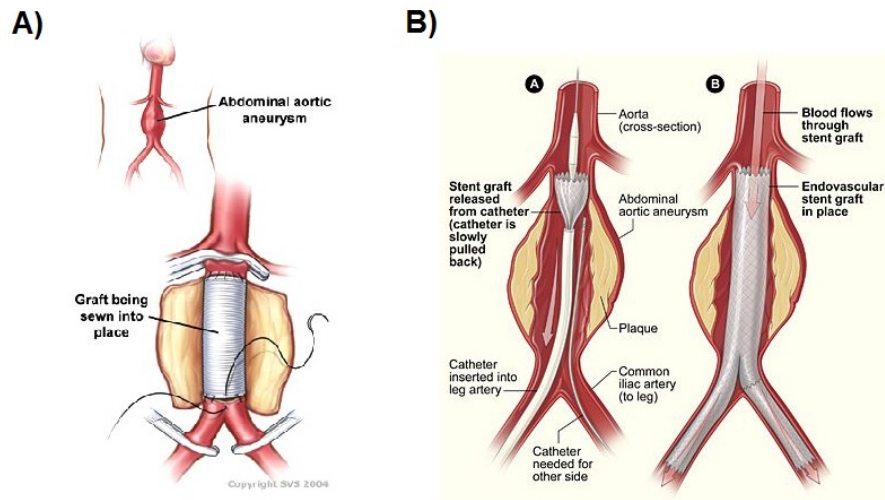


Figure 2.7 Current AAA repair strategies A) open AAA repair; B) Endovascular aneurysmal repair (Adapted from <http://www.vascularweb.org/vascularhealth/pages/abdominal-aortic-aneurysm.aspx>)

2.5 Elastin restorative strategies

Since elastin degradation is a major determinant of AAA growth, its regeneration is critical towards the restoration of normal aortic wall architecture in/around the AAA site. This can then lead to the arrest or stabilization, or even possibly regression of AAA growth, with the newly synthesized elastic matrix combining with the existing elastic matrix to provide the vessel wall with the necessary mechanical properties which help maintain vessel structure and integrity, and also restoring healthy phenotype of the vascular SMCs they would interface with.

2.5.1 Elastic matrix preservation strategies

As discussed in previous sections, one of the major causes of progressively growing AAA is disruption of elastic matrix due to the elastolytic activity due to chronically overexpressed MMPs-2 and -9. Elastin preservative strategies aim to maintain matrix stability by inhibiting proteolytic enzyme production or attenuating/inhibiting their activity using pharmacologic MMP inhibitors, and transcription factor regulators, towards outcomes of slowing matrix degradation, and AAA growth.

Tetracyclines and their derivatives, such as doxycycline (DOX), have been shown to have broad-spectrum inhibitory effects on MMPs [12], including MMPs-2 [13, 95] and -9 [95]. This has been attributed to their inhibition of MMP mRNA transcription [12]. Moreover, studies have demonstrated that DOX treatment inhibits the enzymatic activity of MMP-2 and -9 or pro-MMP activation in certain cell types (vascular SMCs) [96]. Likely due to its MMP-inhibitory effects, DOX has appears to delay the progression of AAAs in induced animal models of AAAs [6], as well as in AAA patients [97], following oral dosing. However, it must also be noted that oral doses of DOX appear to generate dose-dependent side effects [98], with doses in the $\mu\text{g/mL}$ range (typically observed in the circulation following oral dosage) likely inhibitory to elastic matrix synthesis by a variety of cell types [99], including vascular SMCs [100]. Hence, the dose of DOX and its derivatives should be regulated so as to avoid any interference with elastic matrix synthesis and deposition by SMCs. MMPs can also be inhibited endogenously by tissue inhibitor of MMPs (TIMPs); however, the usefulness of TIMPs have been compromised due to issues with large-scale TIMP production, coupled with undesirable outcomes such as cellular apoptosis, which certain TIMPs (e.g., TIMP-3) can induce moreover, since TIMPs are vitally important to regulating various psychological remodeling processes and normal matrix turnover in healthy

tissues, their delivery must be tightly controlled and localized [14]. Serine proteinase inhibitors, such as α_1 -antitrypsin, have been shown to prevent unrestricted and potentially harmful effects of proteases on elastic matrices and protect them from degradation by irreversibly binding to elastases [101]. Exogenous delivery of alternative elastase inhibitors or transfection of vascular SMCs with genes (e.g., antitrypsin gene) that help to enhance *in vivo* production of the elastase inhibitors resulting in inhibited elastin degradation, is another attractive, potential approach [101, 102].

Transcription factors regulate formation of RNA that codes for assembly of proteins in the cell cytoplasm. Transcription factors can be selectively activated or deactivated. In the vascular context, inflammation is specifically regulated by transcription factors that specifically upregulate MMP synthesis and release [15]. Therefore, inhibition of such transcription factors is an approach to treat matrix degradation. However, in the context that MMPs are not globally detrimental in their actions, and indeed serve many useful roles including facilitating normal tissue/matrix turnover. It is not wise to inhibit transcription factors to totally shut off or attenuate MMP synthesis.

Despite the promise held by the techniques discussed above, regression of AAAs is not possible, since elastic matrix is not regenerated actively, a necessary condition for complete AAA growth arrest. Emerging studies in the field have sought to address this problem by focusing on strategies to regenerate elastic matrix.

Chemical crosslinking of vascular elastin is a novel and promising approach to preserve the elastic matrix against enzymatic degradation. Pentagalloyl glucose (PGG), a polyphenolic tannin produced from tannic acid has been shown to attenuate elastic loss from cross-linked/treated blood vessels and preserve the integrity of the elastic lamellae to reduce aneurysm

expansion without particularly increasing inflammation, matrix calcification, or influencing MMP overexpression/activity at the AAA site [103].

2.5.2 Strategies for regenerative elastic matrix repair

Regenerative medicine is defined as “*repair, replacement or regeneration of cells, tissue or organs to restore impaired tissue function resulting from disease, trauma or aging*” [104, 105]. Closely associated with regenerative medicine is the field of tissue engineering, which can manifest itself as *in vitro* or *in vivo* applicable technologies, and broadly defined as “*combination of integral knowledge from physicists, chemists, engineers, material scientists, biologists and physicians to a comprehensive interdisciplinary approach towards development of biological substitutes*” [106]. It is an emerging, and promising alternative to the strategies discussed earlier with respect to preservation of elastic matrices and replacement. The central theme of tissue engineering lies in the ability to utilize living cells in a variety of ways using biomaterial, biomolecule, and mechanical stimuli to repair and/or regenerate tissue. The major goal for vascular tissue engineering is to restore/replace/augment functional and structurally and biologically faithful vascular tissue components. Ideally, ‘engineered’ tissues should provide a microenvironment that replicates that in healthy parenchyma tissue in providing nutrient transport, provides mechanical and phenotypic stability, and maintaining cell-cell and cell-matrix interactions.

Matrix engineering is a sub-field within tissue engineering that specifically aims to *restore, maintain, and improve defective, damage, or injured ECM structures, which is crucial to maintaining tissue homeostasis*. The regeneration of elastic matrix in particular, though critical to vascular homeostasis, has proven to be exceptionally challenging. Due to inherent deficiency of

adult and vascular cells, more so diseased cells to synthesize elastin precursors and assemble them into structurally and biologically–faithful mimics of native elastic matrix, as discussed in section **2.3.2**. An even greater challenge lies in overcoming the above deficiencies within a proteolytic-active/compromised tissue microenvironment that deters new tissue matrix accumulation and compromises its quality. The following sections provide an overview of progress made towards overcoming these problems, and continuing challenges.

2.5.3 *Elastogenic Induction of SMCs*

The presence of GFs in the cellular microenvironment, and their engagement of cellular membrane receptors trigger the activation or inhibition of intracellular signaling proteins and pathways. On these lines, various biomolecular cues are responsible for mediating elastic matrix synthesis. Studies have identified numerous *elastin synthesis stimulators* (e.g., cGMP [107], fetal calf serum [108], insulin-like growth factor 1 (IGF-1) [17, 109]) enlisted in **Tables 2.1 and 2.2** and *elastin synthesis inhibitors* (e.g., ascorbic acid [110, 111], cAMP [107], bFGF [112] and monensin [113, 114]) in **Tables 2.2 and 2.3**.

Studies have demonstrated the effects of TGF- β 1 and IGF-1 in upregulating mRNA expression of tropoelastin by SMCs, and consequent protein translation and matrix deposition [115]. Previous studies in our laboratory have shown the elastogenic effects of TGF- β 1 and IGF-1 when synergistically dosed with hyaluronan oligomers (HA-o – specifically 4-mers and 6-mers) on rat and human aortic SMCs [116-118]. The co-delivery of these factors resulted in increased production of tropoelastin and significant improvement synthesis and alignment of the elastic fibers into matrix structures.

Table 2.1 Biomolecular agents stimulating elastin synthesis and matrix deposition [59]

Biomolecule	Specific Impacts	Cell Type	References
Cyclic GMP	↑ Elastin synthesis in presence of intracellular Ca ²⁺	Ligament fibroblasts	[107]
Fetal calf serum	≥ 5% w/v ↑ elastin synthesis	Ligament fibroblasts	[108]
IGF-1	↑ Tropoelastin and matrix assembly	Aortic SMCs	[17, 109]
Dexamethasone	↑ Tropoelastin synthesis	Ligament fibroblasts	[108]
Bleomycin	↑ Tropoelastin synthesis	Ligament fibroblasts	[108]
Aldosterone	↑ Tropoelastin synthesis and fiber formation	Dermal fibroblasts	[119]
Retinoic acid	↑ Tropoelastin synthesis, ↑ fibrillin	Vascular SMCs, dermal fibroblasts	[120, 121]
Lysyl oxidase	↑ Tropoelastin and matrix assembly	Aortic SMCs	[122]
HA oligomers	↑ Tropoelastin and matrix assembly	Aortic SMCs	[17, 117, 123]
HGF	↑ Tropoelastin synthesis	VFFs	[124]

Table 2.2 Biomolecular agents stimulating and also inhibiting elastin synthesis and deposition [59]

Biomolecule	Specific Impacts	Cell Type	References
HA-long chain	↑ Tropoelastin, ↑ tropoelastin crosslinking, ↑ versican binding, ↓ elastin fiber assembly	Aortic SMCs	[117, 118]
TGF-β1	↑ LOX expression and activity, ↓ MMP-2,-9, ↑ TIMP -1,-2,-3, ↑ elastin synthesis, matrix mineralization at high doses	Aortic SMCs	[16, 21, 116]
Cu ²⁺ ion	↑ Crosslinking, toxic at high doses	Fibroblast, SMCs, Aortic SMCs	[60]

2.6 Elastogenic effects of TGF-β1 in SMC cultures

TGF-β1 is a cytokine which plays a critical role in the cellular expression of elastin and collagen genes [21]. As elucidated in the previous section, prior studies have demonstrated that

Table 2.3 Biomolecular agents inhibiting elastin synthesis and deposition [59]

Biomolecule	Specific Impacts	Cell Type	References
bFGF	↓ Tropoelastin synthesis, ↓ elastin mRNA	Lung fibroblasts	[125]
cAMP	↓ Tropoelastin synthesis, cGMP antagonist	Ligament fibroblasts	[107]
Versican	Release of EBP from cell surface leading to ↓ elastin fiber assembly	Aortic SMCs	[53]
Ascorbic acid	↓ LOX activity, ↓ crosslinking of tropoelastin, ↓ tropoelastin synthesis and matrix assembly	Aortic SMCs, dermal fibroblasts, pulmonary arterial SMCs	[110, 111]
Theophylline	↓ Tropoelastin synthesis, dexamethasone antagonist	Ligament fibroblasts	[108]
Monensin	↓ Tropoelastin synthesis	Ligament fibroblasts, aortic SMCs, chondrocytes	[113, 114]
Bafilomycin A1	↓ Tropoelastin synthesis	Ligament fibroblasts, chondrocytes	[113]
Chloroquine	↓ Tropoelastin synthesis	Ligament fibroblasts, chondrocytes	[113]
NH ₄ Cl	↓ Tropoelastin synthesis	Ligament fibroblasts, chondrocytes	[113]

TGF- β 1 improves matrix assembly by enhancing LOX mRNA expression and its activity [126, 127] and preventing breakdown of existing elastic matrix by downregulating MMP-2 and MMP-9 [19, 21]. It has also been shown to play a role in the upregulation of TIMP 1, 2 and 3 [19]. Other groups have illustrated the overexpression of TGF- β 1 following endovascular gene therapy to improved AAA stabilization in experimental animal models, decrease in infiltration of inflammatory cells, and reduction in MMP-2 and -9 although specific effects on elastin regeneration were not studied [21].

Studies carried out in our laboratory determined the TGF- β 1 dose ranges deemed to have elastogenic effects on vascular SMCs of rat and human, healthy and aneurysmal. The effective

TGF- β 1 dose promoting elastin synthesis tested and reported was 1.0 ng/mL [16, 116], but could certainly be higher or lower, due to known biphasic dose effects of TGF- β 1 [128]. The studied doses of TGF- β 1 were found to improve both tropoelastin synthesis and also matrix deposition and fiber assembly by the vascular SMCs [64, 116], which may be attributed at least in part to the upregulation of elastin at the mRNA and protein levels, as demonstrated by *in vitro* studies by other research groups [129]. The predominant effect of TGF- β 1 on elastic matrix synthesis appears to be the stabilization of elastin mRNA [129], which can be attributed to the presence of a TGF- β 1-responsive element in the human elastin promoter [130].

Previous research from the lab suggests that TGF- β 1 (1.0 ng/mL, 0.25 fg/cell) inhibits undesirable hyper-proliferation of SMCs, and also showed that HA-o, when concurrently provided to cells synergistically enhance the elastogenic effects; tropoelastin synthesis by healthy rat aortic SMCs was increased ~9-fold relative to untreated control types [16]. These studies suggest that TGF- β 1 facilitates tropoelastin recruitment for crosslinking and matrix assembly, as demonstrated by increases in the ratios of matrix to total elastin (i.e.; tropo-matrix elastin). This could be an effect of the observed TGF- β 1-induced increase in LOX protein synthesis and activity. TGF- β 1 does not appear to enhance the extent of crosslinking itself, since desmosine amounts on a per cell basis remained unchanged relative to controls.

However, it must be noted that excessive doses (above 10.0 ng/mL dose) leading to undesirable outcomes/effects, such as matrix mineralization/calcification [16, 20]. Hence, in order to delivery TGF- β 1 doses which stimulate elastogenesis by vascular SMCs, while concurrently avoiding systemic, undesirable effects, there is a need for a delivery system which enables its localized, controlled, and sustained delivery.

2.7 Controlled, localized delivery of therapeutic biomolecules

2.7.1 Nanoparticles as delivery vehicles

As discussed in the previous section, controlled delivery of GFs is essential to enable sustained therapeutic effect, and to reduce adverse side-effects of their systemic-, or over-availability. An overview of advantages of bio-degradable PLGA NPs has been illustrated in **Table 2.4**. This has been accomplished successfully with many therapeutic agents via delivery from polymeric nanoparticles, which serve as vehicular reservoirs for GFs and enable their localized, controlled and sustained delivery at the desired tissue site.

Table 2.4 An overview of advantages of bio-degradable PLGA NPs

Properties	Advantages	References
Usability	Ability to encapsulate macromolecules, nucleic acids, proteins, growth factors, peptides and hormones	[131-133]
Stability	Stability of drug (structure and function) during storage	[134]
Size	Cellular uptake and intracellular trafficking, do not induce inflammatory response by host	[135]
Site specific delivery	Catheter based approach; cellular and tissue targeted delivery: oral, intravascular delivery possible	[132, 135]
SA/V ratio	Enable larger surface area for buffer penetration and result in higher drug release	[136]
Release characteristics	Long term release profiles, non-repeated drug administration	[131]

GFs may be encapsulated or tethered to the NP surface [137], with the former approach being preferred on account of it enhancing the half-life of the GFs, and thereby enabling their enhanced therapeutic effect(s) [137]. A variety of nanoparticle properties play a critical role in mediating the functional effects of these GFs following their delivery.

2.7.2 Nanoparticle characteristics and implications to drug delivery

Nanotechnology, as an emerging field in human medicine, has a wider extent of applications due to its hetero-functionality. There have been many studies with different types of NPs obtained from variety materials, as illustrated in **Table 2.5**. Nanoparticle size is a critical parameter, which mediates their uptake/localization within targeted cells and tissues [137, 138] following their delivery. For example, diseased tissue microenvironments are often characterized by increased permeability due to enhanced vascularity or matrix disruption [139], which improves permeation of these nanoparticles into/at the desired site. Studies have demonstrated that particles larger than 500 nm resulted in events such as phagocytic attack while NP sizes smaller than 100 nm have been shown to elicit immunogenic response [138]. Nanoparticles can be surface functionalized with various chemical groups to modulate their charge, improve binding affinity to specific cellular domains and enhance their intracellular uptake. For example, the cationic functionalization of nanoparticles has been shown to enhance their uptake in the aortic wall [135], as well as intracellular uptake by SMCs, which then has the potential to enhance and sustain their therapeutic effect(s).

The large surface area-to-volume ratio exhibited by NPs enable sustained high rate of release of encapsulated agent(s). The diffusion characteristics and degradation profiles of nanoparticles have been studied widely, which allow us to design them such as to ensure the long term delivery of GFs in controllable pattern into/at targeted sites. For example, higher percentage of glycolic acid in composition of PLGA results in accelerated weight loss of polymer and hence a faster release of the active agent, for example a 50:50 PLGA molecule degrades faster compared to 65:35 PLGA molecule. [136, 140]. In case of molecular weights, a PLGA polymer

with higher molecular weight tends to degrade slowly because of its ability to form long polymeric chains [136, 141].

Table 2.5 Different types of NP matrices and their applications [142]

Material Class	Materials	Application
Natural materials or derivatives	Chitosan, Dextrane, Gelatine, Alginates, Liposomes, Starch	Drug/Gene delivery
Dendrimers	Branched polymers	Drug delivery
Fullerenes	Carbon based carriers	Photodynamics, Drug delivery
Polymer carriers	Poly(lactic acid),	Drug/gene delivery
	Poly(cyano)acrylates,	
	Polyethylenimine	
	Block copolymers	
Ferrofluids	Polycaprolactone	Imaging (MRI)
	SPIONS	
Quantum Dots	USPIONS	Imaging In vitro diagnostics
	Cd/Zn-selenides	
Various	Silica-nanoparticles, mixtures of above	Gene delivery

2.7.3 PLGA as NP matrices

The use of biodegradable polymeric materials in NP based drug delivery systems, particularly provide an advantage serving the desired purpose, without requiring their surgical removal from the body post-drug delivery [131]. Poly(lactide-co-glycolide) (PLGA) is one such biodegradable polymer widely used in field of drug delivery and approved by FDA for clinical use [143]. It is copolymer of poly-lactic acid (PLA) and poly-glycolic acid (PGA) and is synthesized by ring opening copolymerization of cyclic dimers within the monomers [131].

PLGA is an apt polymer for implantation because of its biocompatibility owing to its hydrolytic breakdown/biodegradation into lactic and glycolic acid, both of which are non-toxic to the human body, as they are the natural byproducts of metabolic pathways *in vivo*. The variation of the lactide:glycolide ratio and its molecular weight, provide a wide range of

degradation profiles for PLGA [131, 136], with the surrounding pH and temperature also playing important roles [131, 136]. The degradation primarily occurs in multiple steps via bulk diffusion, surface diffusion, bulk erosion and surface erosion processes [136]. This is illustrated by the fact that PLGA nanoparticles loaded with therapeutics exhibit a biphasic release pattern [136]. The release is initialized by the diffusion of water into the polymer matrix, which leads to the diffusion of therapeutic agent, enabling its release, as well as the hydrolysis of ester bonds within the polymer matrix which leads to the degradation of the polymer [131, 136].

2.7.4 Controlled delivery of TGF- β 1

There is only one published study reported on delivery of TGF- β 1 from PLGA microspheres towards achieving controlled bone regeneration [144]. However, NPs have advantages over microspheres wherein microspheres tend to form fibrotic capsules due to inflammatory response. Most importantly, microspheres are associated with poor cellular uptake and intracellular trafficking when compared to NPs [132]. In the present study, based on our observed *in vitro* elastogenic effects of TGF- β 1 [16, 116], we sought to develop PLGA NPs for (a) enhancing arterial uptake and retention in the aortic wall, (b) enabling controlled, long-term release of TGF- β 1, towards (c) promoting elastin regeneration and/or matrix assembly at AAA sites. More specifically, we determined the *in vitro* release profile of TGF- β 1 from the PLGA nanoparticles as a function of TGF- β 1 loading, b) analyzed its bioavailability and bioactivity and finally c) evaluated its impact on elastin regeneration and elastic matrix formation by aneurysmal rat aortic SMCs. Additionally, the nanoparticles were functionalized with poly-vinyl alcohol (PVA) [145] as a non-ionic stabilizer for the nanoparticle system, which provided the NPs with uniform size distribution [133, 145] and imparts an overall negative charge on nanoparticles

[146]. At the same time, there is also significant potential for surface modification of NPs using cationic amphiphiles such as didodecyldimethyl ammonium bromide (DMAB). The use of these cationic amphiphiles have been demonstrated to not only impart the NPs with a positive surface charge, and enhance their arterial uptake and retention, but also enable their binding with high affinity towards elastin [147, 148] and enhancing elastin fiber crosslinking via upregulation of LOX activity.

CHAPTER III

MATERIALS AND METHODS

3.1 Development and characterization of TGF- β 1 loaded nanoparticles

3.1.1 Reconstitution of TGF- β 1

The recombinant human TGF- β 1 (Catalog no. 240-B; R&D Systems, Minneapolis, MN) was purchased for the purpose of encapsulation within PLGA nanoparticles. The lyophilized TGF- β 1 was activated and reconstituted in acidic buffer as directed by the company and stored at -80°C for long term storage. Briefly, lyophilized TGF- β 1 was activated by 100 μ L of sterile 4mM hydrochloric acid (HCl) containing 0.1% w/v bovine serum albumin (BSA; Catalog no. 0332; Amresco, Inc. Solon, OH). This resultant 100 μ g/mL solution was split into five aliquots of 20 μ L containing 2 μ g each and stored into -80°C. Prior to the use of TGF- β 1, the aliquot was thawed out in ice. The required volume was made up in phosphate buffer saline (PBS; Catalog no. P3813; pH 7.4; Sigma-Aldrich, St. Louis, MO) supplemented with 0.1% w/v BSA.

3.1.2 Formulation of nanoparticles

The formulation of NPs was carried out in two ways; one method included surface functionalization of NPs with PVA (Sigma-Aldrich), which also served as a stabilizer, while the other method involved surface functionalization with DMAB (Sigma-Aldrich). Briefly, poly (*dl*-lactic-co-glycolic acid) NPs (PLGA; 50:50 lactide: glycolide; inherent viscosity of 0.95-1.20 dL/g in hexafluoroisopropanol (HFIP); Durect Corporation, Birmingham, AL) were loaded with TGF- β 1 (R&D Systems, Inc). The NPs were prepared by a double-emulsion/solvent-evaporation technique [131, 136] for both formulations. In case of the PVA-functionalized NPs, 2.5-3.0% w/v PLGA was dissolved in 2 ml of dichloromethane (DCM). As described in the previous section, aliquots containing 1 μ g, 2 μ g and 5 μ g were dissolved in PBS with 0.1% w/v BSA to prepare a total of 100 μ L aqueous TGF- β 1 solution, in each case, which were co-encapsulated with an equal volume of 10% w/v BSA solution [149]. These aqueous TGF- β 1 solutions were emulsified into PLGA solution using a probe sonicator (Q500; QSonica LLC, Newtown, CT) for 1 minute on ice at 20% set amplitude. The water-in-oil emulsion thus formed was further emulsified into an aqueous 0.25% w/v PVA solution using a probe sonicator for 1 minute on ice at 20% set amplitude to form a water-in-oil-in-water emulsion. The second emulsion was stirred using magnetic stirrer for 16 h at room temperature followed by desiccation for 1 h under vacuum to remove any residual DCM. The NPs thus formed were recovered via 3 washing cycles by ultracentrifugation (Beckman Instruments, Inc., Palo Alto, CA) at 35,000 rpm for 30 min at 4°C. The NPs were lyophilized over 48 h to obtain a dry powder. The supernatants obtained during the washing cycles contained residual PVA and unencapsulated TGF- β 1 and were assessed to determine encapsulation efficiency.

NPs prepared with DMAB as stabilizer, were expected to incorporate the surfactant molecules on NP surfaces, and to carry an overall positive surface charge which could enhance the ability of NPs for arterial uptake as described in **Section 2.7.4**. Briefly, 2.5-3.0% w/v 50:50 PLGA was dissolved in 2 mL of chloroform. TGF- β 1 (100, 200 and 300 ng) aliquots were dissolved in PBS containing 0.1% w/v BSA, to make a total of 100 μ l in each case. This aqueous TGF- β 1 was emulsified into the PLGA solution using a probe sonicator for 1 minute on ice at 20% set amplitude to obtain a first water-in-oil emulsion. This was further emulsified into an aqueous 1.0 % w/v DMAB solution using a probe sonicator for 1 minute on ice at 20% set amplitude to form a water-in-oil-in-water (w-o-w) emulsion. The procedure following the formation of w-o-w emulsion is similar to the procedure mentioned previously, in case of PVA-functionalized NPs. The supernatants obtained during the washing cycles contained residual DMAB and unencapsulated TGF- β 1 and were collected for the purpose of evaluating encapsulation efficiency.

However, as will be discussed in detail in Chapter 4, our experiments showed TGF- β 1-loaded NPs functionalized with DMAB, to interfere with detectability of TGF- β 1 via ELISA thus preventing reliable estimation of its release, centric to the goals of this project. Accordingly, the 2 μ g TGF- β 1-loaded, PVA-functionalized formulation was set as solely studied further in cell culture experiments.

3.1.3 Efficiency of encapsulation of TGF- β in nanoparticles

The supernatant solutions obtained during the wash cycles of nanoparticulate synthesis process would be expected to contain un-encapsulated TGF- β 1. Therefore, the supernatants were collected and pooled for evaluation of encapsulation efficiency. The amount of un-encapsulated

TGF- β 1 in the supernatants were quantified using a TGF- β 1 Quantikine[®] enzyme-linked immunosorbent assay (ELISA) kit (Catalog no. DB100B; R&D Systems, Inc). The detected amount of TGF- β 1 in supernatants was subtracted from the total amount of TGF- β 1 added during the encapsulation process, to determine the actual amount of TGF- β 1 encapsulated within the nanoparticles.

3.1.4 Size and surface charge of TGF- β 1 nanoparticles

The measurement of size and surface charge on TGF- β 1 loaded NPs was carried out using a commercial particle sizing system (PSS/NICOMP 380/ZLS, Particle Sizing Systems, Santa Barbara, CA). The size of NPs was determined by measuring the mean hydrodynamic diameter using dynamic light scattering technique (DLS), and the measurements of surface charge were determined via phase analysis light scattering system.

3.1.5 In vitro characterization of release of TGF- β 1 from nanoparticles

The *in vitro* release of TGF- β 1 from NPs was carried out in PBS containing 0.1% w/v BSA over the period of 21 days at 37°C on shaker at 100 rpm. Briefly, 10 mg TGF- β 1-loaded, PVA-functionalized NPs by weight were resuspended in 1 mL release media (PBS with 0.1% BSA) in 1.5 mL polypropylene tubes (n=3) and were placed on a shaker in a 37°C incubator. The tubes were centrifuged (7,000 rpm, 15 min, 4°C) at specific time points (i.e. 4h, 12h, 1d, 2d, 4d, 7d, 10d, 15d, and 21d). The entire volume was collected at each time point and the tube was replenished with equal amount of fresh release media. The release samples thus collected were stored at -20°C until further analysis. The released TGF- β 1 was quantified using TGF- β 1 Quantikine[®] ELISA kit.

The TGF- β 1-loaded, DMAB-functionalized NPs were resuspended in PBS with 0.1% w/v BSA over period of 21 days at 37 °C on shaker at 100 rpm. The procedure for obtaining and storing release samples was similar to PVA-functionalized NPs.

3.2 Determination of TGF- β 1 integrity in release media

The structural integrity/bioavailability of TGF- β 1 released from NPs was confirmed by co-localization of bands corresponding to released TGF- β 1 with those corresponding to exogenous TGF- β 1 standards in western blots [149]. As described in **section 3.1.5**, a suspension containing 10 mg/mL of NPs loaded with TGF- β 1 and 0.1% w/v BSA in PBS, was placed on a shaker at 37°C for 24 h. The released TGF- β 1 was recovered by centrifugation and was concentrated approximately 20-fold through a 10kDa cut-off centrifugal filter (Amicon[®] Ultra, Millipore, Inc., Billerica, MA). This protein solution was loaded on a NuPage[®] 4-12% Bis-Tris Gel (Invitrogen, Inc., Carlsbad, CA; NP0332) under non-reducing conditions, in parallel with a SeeBlue[®] Protein Ladder (Invitrogen, Inc.; LC5925) and TGF- β 1 standards. The proteins on the gel were transferred to a nitrocellulose membrane using the iBlot[®] gel transfer device (Invitrogen, Inc.; IB1001). The membrane was blocked for 1 h using blocking buffer (Li-Cor Biosciences, Lincoln, NE; 927-40000). After blocking, the membrane was immuno-labeled with anti-human TGF- β 1 antibody (Peprotech, Inc., Rocky Hill, NJ; 500-M66) at a dilution of 1:250 v/v in blocking buffer and was placed on shaker for 16 h at 4°C. Finally, the membrane was washed three times in PBST (phosphate buffer saline with 0.01% v/v Tween 20, pH 7.4) and was labeled with IRDye[®] goat polyclonal anti-mouse antibody (Li-Cor Biosciences; 827-08364) at a dilution of 1:20,000 v/v in blocking buffer containing 1:1000 v/v of 10% w/v SDS solution and

Tween-20 each, for 1 h. The protein bands were visualized in an Odyssey imager. The membranes were preserved at 4°C and in dark.

3.3 Determination of functionality of released TGF- β 1

TGF- β 1 is known and has been demonstrated to inhibit the proliferation of mink lung epithelial cells (MLCs) at specific doses. Studies have shown that a 100 pico-molar concentration of TGF- β 1, which is equivalent to 2.5-3.0 ng/mL TGF- β 1, significantly inhibits the proliferative nature of MLCs in 2D culture system [150]. Thus, to confirm the bioactivity of the NP-released TGF- β 1, we sought to demonstrate its ability to inhibit MLC proliferation. The MLCs were purchased from American Type Culture Collection (ATCC, Manassas, VA) and were expanded in Eagle's minimum essential medium (EMEM) supplemented with 10% v/v FBS and 1% v/v Penstrep, cryopreserved according to the literature provided by the company, and thawed for use in experiments.

MLCs were seeded at a density of 12×10^4 cells per well in 6-well plates (A = 10 cm²/well; BD-Biosciences, Franklin Lakes, NJ), (n = 6 for each treatment condition, for each time point). The bioactivity of TGF- β 1 released from PLGA NPs was compared to non-growth-factor added controls, exogenous added TGF- β 1 and blank NPs. Exogenous TGF- β 1 was provided to cells at two different doses, one corresponding to the 3.0 ng/mL 'inhibitory' concentration reported previously, and one corresponding to a concentration of 0.03 ng/mL, previously shown to have no such inhibitory effect on MLCs. Test and control cell cultures were harvested in Pi buffer (50mM disodium hydrogen phosphate, 2mM EDTA, 0.2% w/v sodium azide) at 1d, 4d and 7d (1 plate/condition/time point). Medium was not changed during the culture period. The harvested cell layer was sonicated and stored at -20°C until further assayed.

A fluorometric DNA assay, described in detail further in **Section 3.5.1**, was performed on these harvested cell layers to quantify the cell count at the end of each time point for each treatment condition and confirm the bioactivity of released TGF- β 1.

3.4 Cell Culture

3.4.1 Cell isolation methods

Aneurysmal rat aortic SMCs (EaRASMCs) were isolated from adult male Sprague-Dawley rats (n =3) at 14-days after inducing an AAA via elastase infusion [151]. Our lab has adapted this method for isolating cells [64] and the isolation was carried out by my colleagues Mr. Dennis Wilk and Mr. Partha Deb. To isolate the cells the AAAs were cut open longitudinally and a scalpel was used to scrape off the intimal layer. The exposed medial layer was sectioned out from the underlying adventitial layer, chopped into ~0.5 mm long slices, and washed with warm, sterile PBS. These slices were pooled and enzymatically digested in Dulbecco's minimum essential medium-F12 (DMEM-F12; Invitrogen, Grand Island, NY) cell culture medium containing 125 U/mg collagenase (Worthington Biochemicals, Lakewood, NJ) and 3 U/mg elastase (Worthington Biochemicals) for 30 min at 37 °C, centrifuged (400 g, 5 min), and cultured over 2 weeks in T-75 flasks. The cells were cultured in DMEM-F12 medium supplemented with 10% v/v fetal bovine serum (FBS; PAA Laboratories, Etobicoke, Ontario) and 1% v/v PenStrep (Thermo Fisher, South Logan, UT). The primary EaRASMCs obtained from these tissue explants were propagated over 2 weeks, and passaged when they attained confluence.

3.4.2 Determining in vitro cytotoxicity of TGF- β 1 loaded nanoparticles

The cell cytotoxicity assay was performed on aneurysmal rat aortic smooth muscle cells (EaRASMCs) to determine the maximum non-cytotoxic nanoparticle dose that could potentially be used in 2-D cell culture studies.

The cytotoxic effects of NP addition and NP dose were tested in EaRASMC cultures using a LIVE/DEAD[®] cell viability assay (Invitrogen). Sterile, 2-well Permanox[®] chamber slides (Nalge Nunc International, Rochester, NY) were seeded with 5×10^3 cells per well. The cells were allowed to adhere for 48 h when cultured with DMEM F-12 cell culture medium supplemented with 5% v/v FBS and 1% v/v Penstrep. The TGF- β 1-loaded NPs were added at concentrations of 0.1, 0.2, 0.5 and 1 mg/mL and incubated with the cells for 48 h. For the LIVE/DEAD[®] assay, the cell layers were washed by sterile PBS after complete aspiration of medium. The stain solution containing 1 μ L/mL calcein AM and 2 μ L/mL Ethidium homodimer-1 in PBS was added to each well and incubated for 45 min at room temperature. The cell layers were washed three times, again, by PBS and visualized at 20 \times magnification using an Olympus IX51 fluorescence microscope (Olympus America, Center Valley, PA). The viable cells were visualized as green and dead cells as red.

3.4.3 Experimental design for culture studies for matrix assessment

EaRASMCs were expanded in T-75 flasks at passage 1, in DMEM-F12 medium containing 5% v/v FBS and 1% v/v PenStrep (culture medium). These EaRASMCs were trypsinized and seeded at 6×10^4 cells per well in 6-well plates ($A = 10 \text{ cm}^2$), for matrix assays, PCR and western blot analyses; and 5×10^3 cells per well for immuno-fluorescence studies in 2-

well Permanox[®] chamber slides ($A = 2 \text{ cm}^2$) (Nalge Nunc International). The cells were allowed to adhere to wells over 48 h. Cell layers from one 6-well plate, designated as '0-day cultures', were harvested in Pi buffer to quantify initial seeded cell counts, and other cell layers were further cultured under respective treatment conditions. The effects of released TGF- β 1 on EaRSMCs were ascertained by comparing cell cultures 0.5 mg/mL TGF- β 1 NPs with cultures containing (a) No NPs - culture medium only, (b) exogenous TGF- β 1 equivalent to $\sim 1 \text{ ng/mL}$ over the total cell culture period of 21 days and (c) blank NPs at the concentration of 0.5 mg/mL. Briefly, the volume of medium used for each test culture was 5 mL per well and the spent medium was replaced every 7 days. The culture medium was aspirated out and replenished with fresh culture medium for the non-additive treatment condition. The exogenously added TGF- β 1 was to be supplemented for 7 days until media change, therefore 1.75 ng TGF- β 1 was added to 5 mL culture medium to fulfill the requirement of 1 ng/mL over 21-day period and replenished as described earlier. In case of TGF- β 1 loaded- and blank NPs, entire 5 mL of existing 0.5 mg/mL NP-containing, spent culture medium, from each well, was pipetted out and split into five 1.5 mL-ependorf tubes. These tubes were then centrifuged at 7000 rpm for 15 min at 4°C to recover NPs from the spent medium. The supernatants were aspirated out leaving behind NP pellets, which were each replenished by addition of 1 mL of fresh culture medium. The medium aliquots from the five tubes corresponding to each well were pooled, and pipetted into the respective wells.

At the end of 7 days, the cells were harvested for PCR analysis using RLT buffer (Qiagen, Valencia, CA); which is a cell and tissue lysis buffer. The lysed cell layers were resuspended in 350 μL of RLT buffer and stored at -80°C until RNA isolation and processing samples for PCR.

At the end of 21 days, the cells were harvested for further analysis. The cells used for the estimation of cell proliferation and other matrix assays (elastin and collagen quantification) were harvested in Pi buffer. The culture medium was completely aspirated out and the wells were rinsed three times with sterile PBS to remove any DNases. The wells were then each filled with 1 mL of Pi buffer and scraped using scraper to detach the adhered cells and matrix to ensure complete recovery. This process was repeated two times and therefore a total of 3 ml containing cell layer was pooled and split into three 1.5 mL-ependorf tubes. These tubes were stored at -20°C until further analysis.

Finally, the cell layers to be assessed via western blot analysis were harvested in RIPA buffer (Invitrogen, Inc), containing 1% protease inhibitor (Thermo Scientific, Rockford, IL). Briefly, the culture medium was completely aspirated and 500 μ L of RIPA buffer was added to each well. It is important to note that the cell layers were scraped on ice, collected into 1.5 mL-ependorf tubes and stored in -20°C until further analysis. Prior to their storage, a BCA assay (Thermo Scientific, Inc) was performed on harvested samples to estimate the protein content. Based on the results from BCA assay, single-use aliquots (~50 μ L) were made and stored at -20°C.

3.5 Matrix Assays

3.5.1 DNA Assay

The effect of TGF- β 1 loaded NPs on proliferation of EaRSMCs was determined by measuring the total DNA content in the cell layers and its comparison with the control cases, via a fluorometric assay as described by Labarca and Paigen [152]. Briefly, the cell layers were harvested at 1d time point and 21d time point of culture period, in Pi buffer. The harvested cell

layers were sonicated on ice for a total of 30 sec, with alternating 5 sec pulse and 5 sec pause. DNA standards used were the serial dilutions from 10 $\mu\text{g}/\text{mL}$ stock solution of calf thymus DNA. Briefly, 100 μL of sample was diluted in 395 μL of Pi buffer and mixed with 505 μL of 2 $\mu\text{g}/\text{mL}$ Pentahydrate (bis-benzimide) (Hoechst 33258; Invitrogen, Inc) solution in Pi buffer. The sample and standard tubes were vortexed well and incubated at room temperature in dark for 30 min. A 200 μL aliquot was pipetted out in each well of 96-well, fluorescence plate, and read at excitation set to $\lambda = 356$ nm and emission set to $\lambda = 458$ nm. The cell layers were thus assayed for DNA content and the cell density was therefore calculated assuming 6 pg of DNA/cell [152].

3.5.2 *Fastin Assay*

The total elastin content in the cell layer (alkali-soluble and insoluble matrix fractions) was quantified using a Fastin elastin assay kit (Biocolor, Inc, UK). The cell layers were harvested after 21 days of culture and resuspended in Pi buffer. These cell layer fractions were then sonicated on ice for 30 sec in all, alternating 5 sec pulse and 5 sec pause, to homogenize the cell layer. The resultant suspension was centrifuged at 2500 rpm for 10 min and Pi buffer was subsequently aspirated. The pellet was suspended in 1 mL of 0.1N NaOH and digested for 1 h at 98°C. The suspension was centrifuged at 10,000 rpm for 10 min, and supernatant containing alkali-soluble elastin was recovered ensuring that the pellet remained undisturbed. The pellet was then suspended into 1 mL 0.25M oxalic acid and digested at 95°C for 1 h, to convert the insoluble fraction of elastin into soluble, α -elastin detected by Fastin assay kit. The resultant suspension was passed through 10-kDa cut off centrifugal filters (Amicon[®] Ultra, Millipore, Inc., Billerica, MA) and the retentate (containing alkali-insoluble elastin) was collected by reverse

centrifugation, and labeled as insoluble elastin. The digested elastin samples, soluble and insoluble fractions, were stored at 4°C.

The sample volume used to perform the Fastin assay was 100 μL from the elastin samples isolated previously. It is important to note that the volumes at the end of filter centrifugation were not equal. Therefore, the volume in all the tubes were made up to 100 μL . Briefly, 100 μL of samples for all the test conditions was mixed with 100 μL of elastin precipitating reagent in a 1.5 mL-ependorf tube. The suspension was vortexed and incubated for 15 min at room temperature. The tubes were then centrifuged at 14,000 rpm for 20 min in a microcentrifuge. The content of the tubes was then decanted into a glass beaker and the tubes tapped on a paper towel to ensure maximum decantation. The upper sides of the tubes were cleaned with a Q-tip and it was ensured that the contents would be less than 25 μL . Later, 500 μL of the elastin dye was added to the tubes and incubated for 90 min at room temperature. At the end of this incubation period, the tubes were again centrifuged at 14,000 rpm for 20 min. The contents in the tube were dried out by decantation procedure mentioned above. A reddish-brown colored pellet, visible at the bottom of the tubes, was dye bound elastin. The tubes were then filled with 250 μL of dye dissociation agent, and vortexed well. The entire 250 μL volume was pipetted out and read in a clear, absorbance 96-well plate via spectrophotometer (SpectraMax M2, Molecular Devices, Inc., Sunnyvale, CA) at $\lambda = 513 \text{ nm}$. Note that the sample absorbances were read in triplicate, used to estimate elastin amounts per well, and then normalized to corresponding cell counts from DNA assay to provide accurate comparison between treatment conditions.

3.5.3 *Hydroxy-Proline Assay*

A hydroxyl-proline (OH-Pro) assay was used to estimate the collagen content within test and control cell layers. On the grounds of presence of 4% w/w OH-Pro in soluble elastin, 500 μ L of soluble elastin isolated, as described in previous section, was further digested to obtain OH-Pro residues. The solubilized elastin in 0.1N NaOH was neutralized by adding 500 μ L of 6N hydrochloric acid (HCl) in 2 mL glass vials. The tubes were tightly capped and placed in a heating block for 16 h set at 110°C. The lids of the tubes were then removed and dried with nitrogen gas treatment for approximately 90 min, leaving a white precipitated residue at the bottom of vials. These vials were then reconstituted with 100 μ L of de-ionized water and stored at 4°C until assay.

The standards were prepared as a serial dilution of 6 μ g of OH-Pro from a 1 mg/mL OH-Pro stock solution. Briefly, 20 μ L of the OH-Pro isolated samples from cell layers and standard samples were added to glass tubes containing 500 μ L deionized water. Chloramine-T reagent was prepared by adding 0.353 g of Chloramine T in 20 mL of 50% v/v n-propyl alcohol, and made up to 100 mL using OH-Pro buffer (50 mg citric acid, 12 mL glacial acetic acid, 120 g sodium acetate hydrate, 24 g sodium hydroxide, 300 mL n-propyl alcohol, made up to 1.5 L, pH 6.0). Chloramine T reagent (250 μ L) was added to the tubes, vortexed and incubated at room temperature for 15 min. Thereafter, 250 μ L of Ehrlich's reagent (2.25 g p-dimethyl-amino-benzaldehyde, 9 ml n-propyl alcohol, 3.9 ml of 70% perchloric acid) was carefully added to the suspension in tubes and vortexed, in a chemical hood and placed into a heating block for 15 min at 60°C. The samples with higher collagen content would appear to turn yellow to red. A 250 μ L aliquot of these solutions was pipetted onto a clear 96-well plate and read for absorbance at $\lambda =$

558 nm [153]. The total collagen content was then calculated on the basis of the 13.2% OH-Pro content of collagen [154], and normalized to the DNA content of corresponding cell layers.

3.6 Immunofluorescence detection of elastic matrix assembly proteins

Immunofluorescence labeling studies were carried out to visualize the deposition of elastin, fibrillin and LOX by EaRASCs in matrix through the culture period, and support other quantitative assay results. As described previously, 8×10^3 EaRASCs were seeded in sterile, 2-well Permanox[®] chamber slides (Nalge Nunc International) and treated with respective test conditions for 21 days, for immunofluorescence studies.

After 21 days of culture, the cell layers were fixed with 4% w/v paraformaldehyde and blocked using blocking buffer (5% goat serum in PBS) for 1 h. These slides were then treated with rabbit polyclonal antibodies against elastin (Catalog no. ab21610; Abcam, Cambridge, MA), fibrillin-1 (Catalog no. ab53076; Abcam) and LOX (Catalog no. ab31238; Abcam), all at 1:100 v/v dilutions overnight at 4°C. The slides were washed with PBS and treated with 1:1000 v/v dilution of Alexa Fluor[®] 633-conjugated goat anti-rabbit secondary antibody (Invitrogen, Inc.; A-21070). The cell nuclei were stained using a fluorescent nuclear stain 4, 6-diamino-2-phenylindole dihydrochloride (DAPI) contained in the mounting medium (Vectashield; Vector Labs, Burlingame, CA).

3.7 Western Blot for LOX

Western blot analysis was performed to semi-quantitatively assess effects of NPs with and without TGF- β 1, on LOX protein synthesis in EaRASC cultures. The cell layers from the test conditions described in **Section 3.4.3**, were harvested in RIPA buffer. Based on the results

from BCA assay, an equivalent of 4 μ g of protein was loaded in 4-12% Bis-Tris Gel (Invitrogen, Inc.). The proteins were transferred to nitrocellulose membrane using iBlot system (Invitrogen, Inc.). The membrane was then blocked with blocking buffer (Li-Cor Biosciences) for 1 h, at room temperature. The membrane was then treated with primary antibodies (1:200 v/v anti-LOX (SantaCruz Biotechnology, Inc Santa Cruz, CA; SC32410), 1:1000 v/v anti-actin (Sigma Aldrich; A3853), 1:1000 v/v Tween 20) in blocking buffer for 16 h at 4°C. The membranes were washed in PBST thrice before treating it with secondary antibody (1:15,000 v/v IRDye[®] donkey polyclonal anti-goat (Li-Cor Biosciences), 1:20,000 v/v IRDye[®] goat polyclonal anti-mouse (Li-Cor Biosciences), 1:1000 v/v 10% SDS solution, 1:1000 v/v Tween 20) in blocking buffer for 1 h, at room temperature. Finally, the membranes were washed three times in PBST and visualized under Odyssey Imager.

3.8 Real Time Polymerase Chain Reaction (RT-PCR) for quantifying mRNA expression of proteins associated with elastin synthesis processes

3.8.1 Isolation of mRNA

The cell layer suspension was diluted with 350 μ L of 70% v/v ethanol. The resultant 700 μ L of cell layer suspension was transferred to RNeasy spin column and centrifuged for 30 sec. The flow-through was discarded from the collecting tube and 700 μ L RW1 was added to the spin column. This suspension was centrifuged for 15 sec at 10000 rpm. The flow-through was discarded again discarded and 500 μ L of 1 \times RPE buffer was added to the spin column. This was centrifuged for 15 sec at 10000 rpm and 500 μ L of 1 \times RPE buffer was again added to the spin column. The 15 sec centrifugation at 10000 rpm was repeated and the flow-through was discarded. The spin column was transferred to another collecting tube. The spin column was

centrifuged for 1 min at 14000 rpm. Later, the spin column was again transferred to a 1.5 mL collecting tube and 30 μ L of DEPC water was added to spin column. This was centrifuged at 14000 rpm for 1 min. The filtrate (\sim 30 μ L) was added back to spin column to ensure complete mRNA recovery and centrifuged at 14000 rpm for 1 min. The filtrate was stored at -80 $^{\circ}$ C.

3.8.2 *mRNA quantification*

The mRNA was quantified using the Ribo-green assay kit (Invitrogen). Briefly, 2 μ L of isolated mRNA was diluted with Tris-EDTA (TE) buffer to make a 100 μ L of total assay sample, and pipetted into an opaque, fluorescence 96-well plate. A 100 μ L aliquot of working ribo-green reagent (diluted in TE buffer) was added to each assay sample in the 96-well plate. The samples were quantified using a standard curve obtained from the serial dilutions of 2 μ g/mL of mRNA standards, which were supplied with the kit. The fluorescence of samples was read at excitation of $\lambda = 480$ nm and emission of $\lambda = 520$ nm.

3.8.3 *Reverse transcription of mRNA*

The reverse transcription of mRNA results in cDNA that serves as template in amplification process of RT-PCR. Approximately 400 ng of mRNA, mixed with recommended concentrations of reverse transcriptase (RTase) and reaction buffer cocktail, was reverse transcribed using iScript cDNA synthesis kit (Biorad Inc, Hercules, CA). The reaction mixture was placed in a thermocycler and converted to cDNAs.

3.8.4 RT-PCR

RT-PCR was used to evaluate the gene expression of proteins of interest, associated with elastin assembly process, in cultures treated with TGF- β 1 NPs and compared to untreated cultures. Specifically, this study aimed to focus on the gene expression of elastin, collagen type-1, LOX, fibrillin-1 and fibulin-5. The elastin (*Eln*) [16], collagen (*Colla1*) [155] and fibrillin-1 (*Fbn1*) primers used for amplifying the cDNAs in the RT-PCR, and were designed by senior colleague in our lab, Dr. Chris Bashur, while the 18S (house-keeping gene; *Rn18s*), fibulin-5 (*Fbln5*) and LOX (*Lox*) primers were commercially purchased from Real Time Primers, LLC (Elkins Park, PA).

Table 3.1 Proteins associated with elastin synthesis and their primer sequences

Protein	Forward primer sequence 5' - 3'	Reverse primer sequence 5' - 3'	Size (bp)
<i>Eln</i>	CCTGGTGGTGTACTGGTATTGG	CCGCCTTAGCAGCAGATTTGG	60
<i>Colla1</i>	GAGGGCGAGTGCTGTCCTT	GGTCCCTCGACTCCTATGACTTC	74
<i>Fbn1</i>	ATAAATGAATGTGCCAGAATCCC	ACTCATCCTCATCTTTACACATCC	132
<i>Fbln5</i>	CGAGGGTCGAGAGTTCTACA	CAGAACGGATACTGGGACAC	186
<i>Lox</i>	AGACGATTTGCCTGTACTGC	ATAGGCGTGATGTCCTGTGT	219

Briefly, 2 μ L of cDNA, which is equivalent to 8 ng cDNA, was mixed in appropriate concentrations of primers and 10 μ L of Power-SYBR[®] Green Master Mix (Applied Biosystems, Foster City, CA). The total volume of the resulting solution was made up to 20 μ L by nano-pure RNase free water. All the samples (n = 6/test condition) were processed in duplicates and were read in ABI 7500 Real Time PCR System (Applied Biosystems). The instrument measured the fluorescence of SYBR[®] Green bound to amplified DNA. The gene expression profiles were analysed using liner regression of efficiency method [156] using a specifically developed MATLAB code [157]. Gene expression of 18s ribosomal RNA served as an internal control (house-keeping gene) to normalize the results to report the final DNA copy numbers.

CHAPTER IV

RESULTS AND DISCUSSION

4.1 Characterization of NPs

As described in chapter 3, the choice of polymer and solvents used, emulsion stirring rate, and NP fabrication technique (e.g., single- or double-emulsion technique) play a critical role in determining the size of NPs and the encapsulation efficiency of drugs within [136]. Size and surface charge characteristics of NPs have been shown to mediate their uptake within various cell and tissue types. For our long-term application (i.e., aneurysm treatment) we deemed it essential to generate NPs of hydrodynamic sizes smaller than 500 nm to avoid phagocytic attack, and greater than 100 nm to avoid immune response [138]. Within this size range, smaller NP sizes would be preferred, since they would provide the NPs with a higher surface to volume ratio that would enable enhanced buffer penetration and consequently higher levels of drug release [158]. Our TGF- β 1 loaded NP formulations, surface functionalized with PVA, resulted in sizes ranging between 296 nm and 352 nm. However, in accordance with other studies, the NP

formulations generated using DMAB as a surfactant resulted in smaller sized NPs ranging between 236 and 281 nm [133, 146]. It is important to observe that the NP size tended to decrease with increasing TGF- β 1 loading, and could possibly be attributed to better compaction/lower porosity of the polymer/drug-matrix and hence lesser swelling in aqueous media. Studies by Murakami et. al. [159] showed NP swelling ratio (hydrated to dry NP volume) to correlate with high initial release, which in turn is inversely correlated to active agent loading. Our release data shown in **Section 4.2**, agrees with this trend.

PVA, a non-ionic surfactant, is widely adopted in NP formulation to impart an overall negative surface charge (ζ -potential) and to stabilize the emulsion generated during NP formulation [160]. The size and ζ - potential for blank NPs and TGF- β 1 NPs is listed in the **Table 4.1**. The average ζ -potential for PVA-functionalized NPs loaded with TGF- β 1 was -27.5 mV, which was comparable to -28 mV ζ -potential, achieved by other publications using PVA functionalized NPs [161]. The NPs formulated with DMAB as a surfactant expectedly imparted an overall positive surface charge to the NPs (ζ -potential = +32.2 mV, see **Table 4.2**), which would be important from the standpoint of enhancing their arterial uptake [161].

Table 4.1 Data showing size (n = 6), and surface charge (ζ - potential) (n = 6) for blank and TGF- β 1-loaded PLGA NPs, surface functionalized with PVA. Also shown are the efficiencies of encapsulation of TGF- β 1 within the NPs (n = 3). Data are represented as mean \pm SD.

	Blank NPs	TGF- β 1 loaded NPs		
		1 μ g	2 μ g	5 μ g
Size (nm)	275.6 \pm 28.8	295.8 \pm 5.1	351.7 \pm 9.9	347.4 \pm 40.3
ζ- potential (mV)	-30.3 \pm 2.3	-28.1 \pm 2.0	-25.5 \pm 2.8	-25.9 \pm 3.0
Encapsulation efficiency (%)	NA	85.7 \pm 1.2	73.8 \pm 14.6	91.4 \pm 3.0

Table 4.2 Data showing size (n = 6), surface charge (ζ - potential) (n = 6) and efficiencies of encapsulation of TGF- β 1 within the NPs (n = 1), surface functionalized with DMAB. Data are represented as mean \pm SD.

	TGF-β1 loaded NPs		
	0.1 μg	0.2 μg	0.3 μg
Size (nm)	280.5 \pm 11.4	265.5 \pm 18.5	236.3 \pm 5
ζ- potential (mV)	32.9 \pm 2.2	30.1 \pm 4.1	33.5 \pm 2.5
Encapsulation efficiency (%)	68.3	74.5	81.2

The encapsulation efficiency of TGF- β 1 NPs was calculated by estimating the amount of unencapsulated TGF- β 1 in the supernatants obtained upon pelleting TGF- β 1 encapsulated NPs by ultracentrifugation. Our studies demonstrated high encapsulation efficiencies for both PVA- and DMAB-formulated NPs. After subtracting the estimated amount from the initially loaded TGF- β 1, the overall encapsulation efficiency ranged between 74 \pm 15 % and 91 \pm 3% for PVA-formulated NPs, while they ranged between 68.3 % and 81.2 % for DMAB-functionalized NPs. These encapsulation efficiencies are high compared to other studies encapsulating TGF- β 1 within micro-particles, which reported entrapment efficiencies of 25-50% [162, 163].

4.2 Release of TGF- β 1 from PLGA NPs

Nanoparticles loaded with active agents release the drug first upon hydrolytic surface degradation and later, through aqueous infiltration into NP matrix, followed by bulk diffusion. Methods like HPLC [164], and UV-spectrophotometry [165] are used for *in vitro* detection of the NP-released active drugs in aqueous reservoirs. When growth factors are instead encapsulated within nanoparticles and microparticles, their release is detected or quantified using ELISA [144,

160]. This technique has the advantage of being highly specific for detecting proteins of interest. In this study, the amounts of TGF- β 1 detected at various time points were plotted together to obtain a cumulative TGF- β 1 release curve, as shown in **Figures 4.1** and **4.2**.

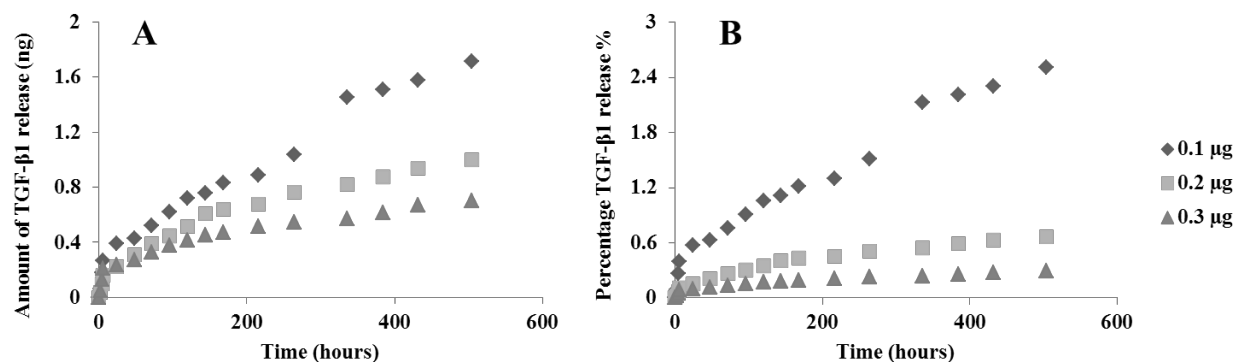


Figure 4.1 Cumulative release curves of TGF- β 1 from NPs loaded with TGF- β 1 over 21 days, surface functionalized with DMAB ($n = 1$). A) Represents the absolute amounts of TGF- β 1 released by NPs in 1 mL of release media; B) Represents the percentage release of encapsulated TGF- β 1 in NPs

TGF- β 1 was released from 0.4 mg/mL concentration of NPs formulated with DMAB, in PBS and quantified using ELISA. As illustrated in **Figure 4.1**, the overall TGF- β 1 released over the period of 21 days was approximately 2.5% of the total TGF- β 1 encapsulated. It should be noted that the release was higher in NPs with lower TGF- β 1 loading density (0.1 μ g). The cumulative release curves appeared biphasic as others have also shown with other active agents released from PLGA NPs [159]. A high initial burst of approximately 1 ng in the first 24 h followed by a flattening ‘lag’ phase, and further followed by a second phase on relatively rapid increase at day 15. The initial burst is attributable to release of physically adsorbed drug on the NP surface, and the delayed release phase to release of covalently bound/entrapped drug within the PLGA matrix released as the NP degrades. Despite this encouraging result, a problem encountered was that DMAB contributes to false positive detection of TGF- β 1 via ELISA. For

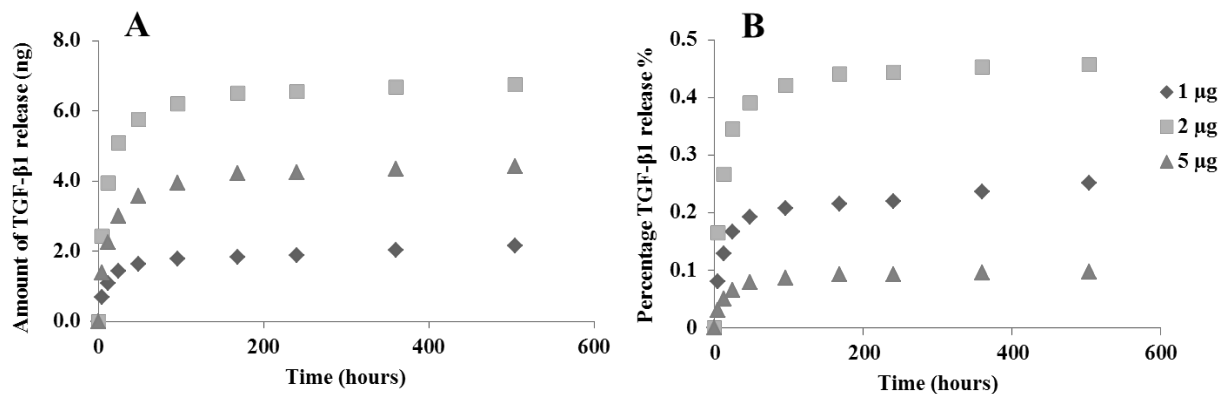


Figure 4.2 Cumulative release curves of TGF-β1 from NPs loaded with TGF-β1 over 21 days, surface functionalized with PVA (n = 3). A) Represents the absolute amounts of TGF-β1 released by NPs in 1 mL of release media; B) Represents the percentage release of encapsulated TGF-β1 in NPs

example, a 0.01% w/v DMAB solution in PBS was read as equivalent to 0.35 ng of TGF-β1, when processed on the ELISA plate. Due to this, it led into artificial ramping up of TGF-β1 detected. Thus, the amount of TGF-β1 released from DMAB-PLGA NPs as estimated by ELISA, was deemed unreliable. On this account, the DMAB-NPs were deemed unsuitable for use in subsequent cell culture experiments, wherein the provided TGF-β1 dose would required to be known. Differently, we did not observe any such false positive detection of TGF-β1 when a solution containing 0.01% w/v PVA was subjected to ELISA. Accordingly, the effects of NP-released TGF-β1 on cells were further investigated using only PLGA-NPs formulated with PVA. Considering the lower detection limit and high specificity of ELISA technique for TGF-β1, TGF-β1 released from a 10 mg/mL NP suspension in PBS was in the detectable range of the commercially purchased ELISA kit. The highest release of TGF-β1 (6.8 ± 0.1 ng in release media) was detected from NPs loaded with 2 μg of TGF-β1, which was equivalent to 0.5% of total TGF-β1 encapsulated in the NPs. The overall release of TGF-β1 was deemed low and accordingly none of the TGF-β1 loadings, however, was found to release the equivalent of 1.0

ng/mL over 2 days to match the exogenous TGF- β 1 dose shown by our group to have elastogenic effects in previous publications [16]. The release of TGF- β 1 from the PLGA NPs could potentially be limited due to the high molecular weight of PLGA (117 kDa), or its high lactide content (50%), both of which could prolong degradation and hence release of active agent. Future studies will seek to modulate these parameters to be able to enhance TGF- β 1 release levels as required.

4.3 Bioavailability and Structural integrity of released TGF- β 1

The structural integrity of NP-released TGF- β 1 was confirmed by comparing its co-localization with a band generated by exogenous, un-encapsulated TGF- β 1 on a western blot gel and detected using an anti-TGF- β 1 antibody. The bands corresponding to NP-released TGF- β 1 and exogenous TGF- β 1 were both detected and migrated the same down a polyacrylamide gel (see **Figure 4.3**) demonstrating that released TGF- β 1 did not undergo any structural changes and

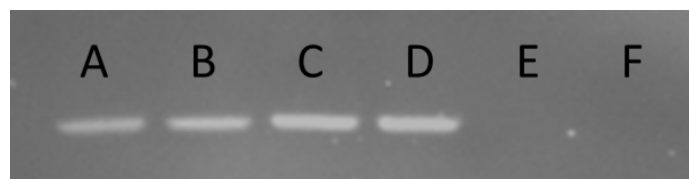


Figure 4.3 Western blots of released TGF- β 1 (25 kDa). Lanes A and B (duplicates) contain TGF- β 1 before entrapment; lanes C and D contain TGF- β 1 released from NPs; and lanes E and F contain release media from Blank NPs.

fragmentation. It is important to note that the bands of released TGF- β 1 are brighter than the 1 ng/lane positive control bands, suggesting a fairly high TGF- β 1 release in a 24 hour period, which we also deemed from ELISA measurements.

4.4 Bioactivity of released TGF- β 1 in Mink Lung Cell cultures

It has been shown that TGF- β 1 inhibits the proliferation of cells derived from epithelial, endothelial, hematopoietic, and neural tissues [150]. More specifically, 100 pM TGF- β 1, equivalent to a concentration of \sim 3.0 ng/mL, has been reported to significantly inhibit the proliferation of mink lung cells (MLCs) in culture [150]. We sought to assess the inhibitory effects of TGF- β 1 released from NPs on MLCs, to confirm its continued bio-functionality/activity.

As described in **Section 3.3**, the MLC cultures were dosed with TGF- β 1 NPs at a concentration of 0.5 mg/mL. Their effects were compared with separate cultures wherein blank NPs were provided at the same concentration and a known non-inhibitory dose (0.03 ng/mL, equivalent to 1 pM) of exogenous TGF- β 1. In addition to these negative controls, there was an untreated treatment condition as well. Cultures dosed with known inhibitory TGF- β 1 dose (3.0 ng/mL) served as a positive control. Our experiment showed cell counts for the non-additive treatment condition, non-inhibitory dose of exogenous TGF- β 1, and blank NP-treatment conditions to not differ at all assay time points (days 1, 4 and 7 post-seeding). While untreated MLCs at day 7 showed 3.2 ± 0.2 -fold increase in number compared over initially seeded cell counts, cells treated with 3.0 ng/mL of exogenous TGF- β 1 exhibited a more limited 2.2 ± 0.1 -fold increase. This suppressive effect of MLC numbers upon treatment with exogenous TGF- β 1

(100 pM or 3.0 ng/mL) relative to untreated controls was maintained at all studied time points, as shown in **Figure 4.4**. In case of MLCs treated with TGF- β 1 loaded NPs, the effects were not as pronounced as the 100 pM exogenous TGF- β 1-treatment condition, but significantly different ($p < 0.001$) than outcomes observed in the negative controls and blank NP treated condition. There was only 1.4 ± 0.1 fold increase in cell counts cultures treated with TGF- β 1 releasing NPs with

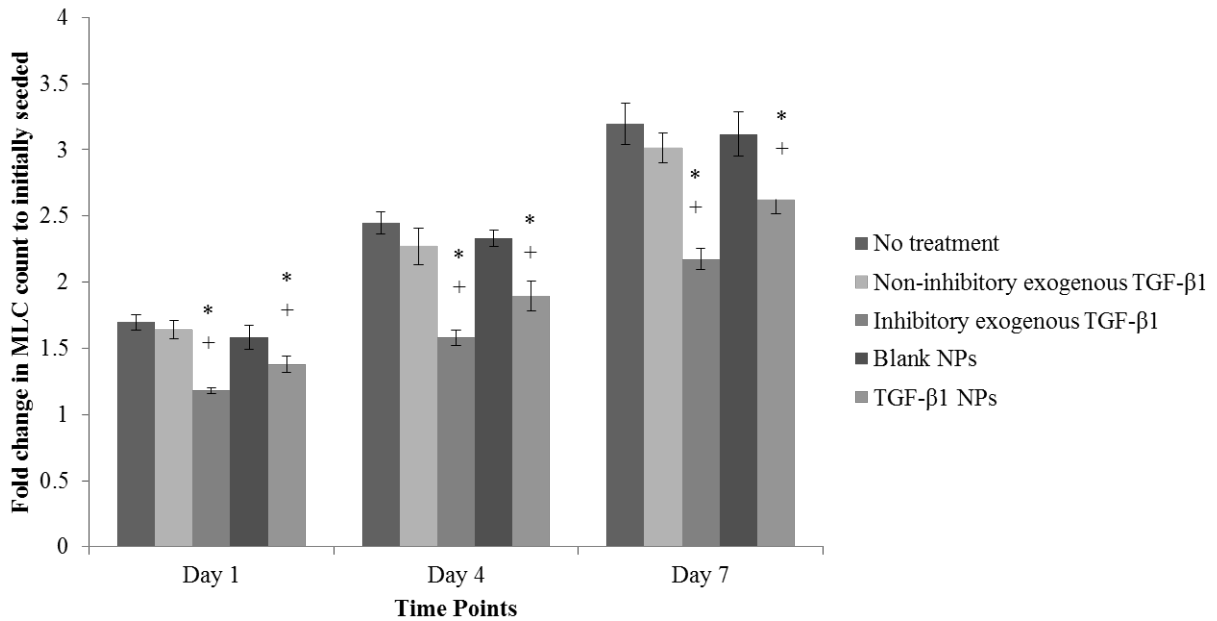


Figure 4.4 Effect of TGF- β 1 and control treatment conditions on proliferation of MLCs, seeded at 12×10^4 cells per well ($n = 6$ wells/case). Results shown represent mean \pm SD of fold increases in cell number relative to that at seeding. Significant differences versus untreated and blank NP treated cultures are indicated as * and + respectively, and was deemed for $p < 0.05$.

after 1 day of exposure, relative to 1.7 ± 0.1 ($p < 0.001$) fold increase observed for the no treatment cultures, and 1.6 ± 0.1 ($p < 0.011$) fold increase for the blank NP supplemented cultures. The suppressive effects of NP-released TGF- β 1 on MLC proliferation were maintained at longer time points also. This clearly demonstrates the inhibitory effects of released TGF- β 1 on MLCs. Conclusively, this experiment showed the existence of active TGF- β 1 released from NPs

and the inhibitory effects were attributed as measure of its bio-functionality, released in cell culture media.

4.5 Lack of cytotoxic effects of TGF- β 1 NPs on EaRASCs

The concentration-dependent cytotoxicity of PLGA NPs loaded with TGF- β 1 was assessed using a LIVE/DEAD[®] viability assay kit as described in **Section 3.4.2**. The assay components include calcein AM that stains viable cells to fluoresce green, while ethidium homodimer-1 (Ethd1) stains dead cells to fluoresce red. The mechanism of this assay is dependent on intracellular esterase activity of cells which enzymatically converts the calcein AM to fluorescent calcein, and Ethd1 permeates through membranes of dead cells to bind to the nucleic acids and undergo 40-fold fluorescence enhancement.

The representative images obtained after LIVE/DEAD[®] assay carried out on EaRASC cultures using NPs loaded with TGF- β 1 at concentrations (0.1, 0.2, 0.5 and 1 mg/mL and untreated control) are shown in **Figure 4.5**. The LIVE/DEAD assay outcomes showed $99 \pm 1.8\%$ of cells to be viable when cultures were treated with NPs at concentrations 0, 0.1, 0.2 and 0.5 mg/mL. For NP concentration of 1.0 mg/mL, cell viability was $97.8 \pm 3.4\%$, which was however, not significantly different from a statistical standpoint from cultures treated with lower NP doses. Based on these outcomes, we confirmed that cell culture studies conducted with an NP concentration of 0.5 mg/mL, would not adversely impact cellular health and viability.

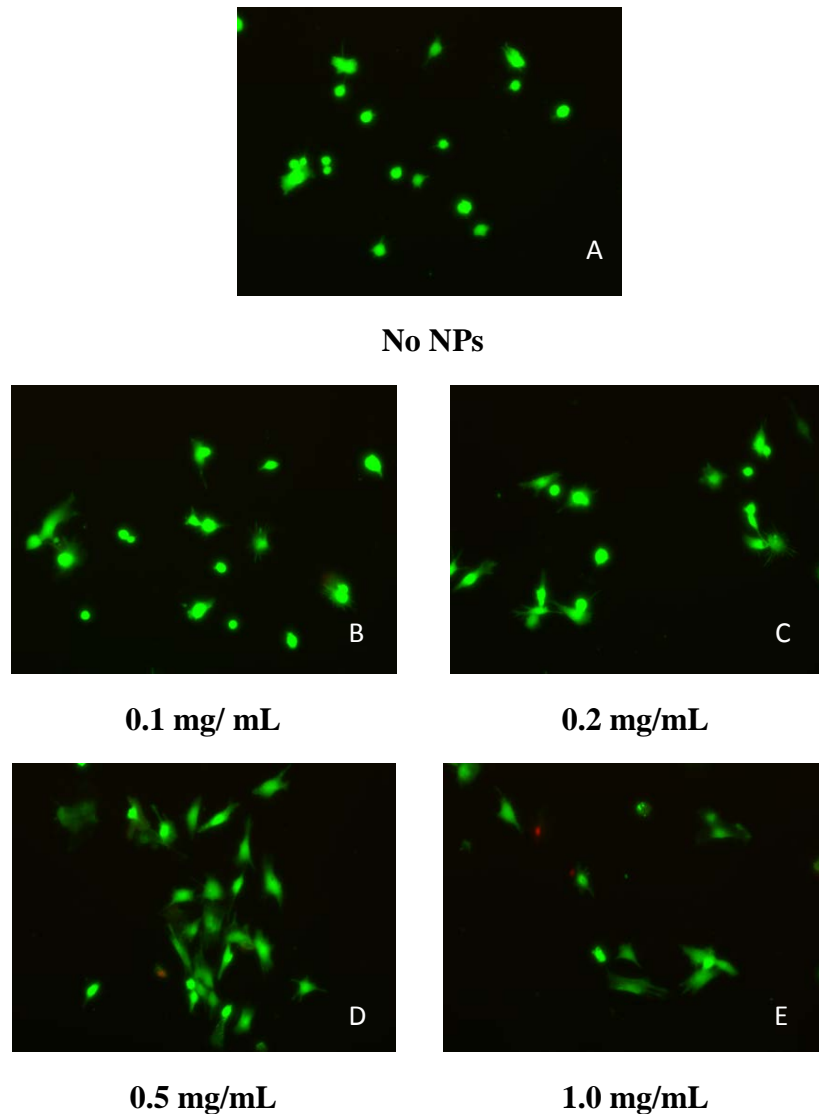


Figure 4.5 Results from LIVE/DEAD[®] assay. Viabilities in all cultures, treated and untreated were > 99%, except for 1.0 mg/mL of NPs (E) where it was ~ 97%

4.6 Effect of TGF-β1 release from NPs on EaRASC proliferation

The fluorometric DNA assay was carried out on cell layers harvested on day 0 samples and day 21 samples for all the treatment conditions, as described in **Section 3.5.1**. The average cell counts at day 0 were $(3.3 \pm 0.6) \times 10^4$ cells per well (n = 6 per test case).

The average fold increase in cell number at the end of 21 days compared to initial adhered cell counts for all the treatment conditions was 4.1 ± 0.4 . It must be noted that the cell counts obtained from exogenous TGF- β 1 and TGF- β 1 NP treatment conditions were significantly lower than the untreated condition ($p \ll 0.001$), as shown in **Figure 4.6**. This result could be attributed to the ability of TGF- β 1 to arrest the proliferation of EaRSMCs, which could be useful to attenuate potential hyper-proliferation of activated SMCs involved in tissue remodeling at the AAA sites, when the TGF- β 1 NPs are ultimately delivered as therapy [116, 166].

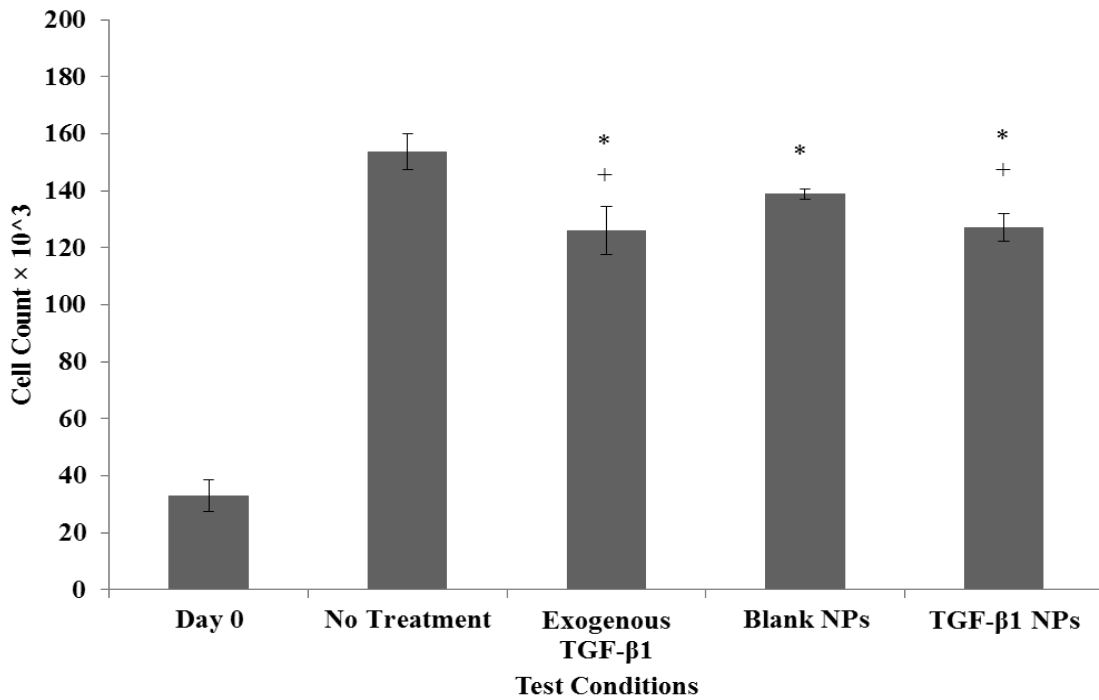


Figure 4.6 Results of DNA assay showing EaRSMCs count initially seeded and after 21 days of treatment with NPs loaded with TGF- β 1 and other control test conditions. Shown are the mean \pm SD of counts determined from $n = 6$ cultures/case. Significance of differences versus the no treatment conditions and blank NPs at 21 days are indicated as * and + respectively, and was deemed for $p < 0.05$.

4.7 Matrix Assays

4.7.1 *Fastin Assay*

The quantification of elastin deposited by EaRASMCs upon exposure to NPs loaded with TGF- β 1 and other control cases was estimated using a Fastin assay, as described in **Section 3.5.2**. The results from these studies for all the treatment conditions are illustrated in **Figure 4.7**.

As described earlier, the TGF- β 1 released from NPs was considerably lower than the exogenous dose of 1.0 ng/mL TGF- β 1, which was previously shown to mediate elastogenic induction of EaRASMCs [116]. As a result, the amounts of alkali-insoluble elastin generated in cultures of treated with TGF- β 1 loaded NPs were not significantly higher compared to the other treatment conditions/controls (**Figure 4.7**). The alkali-insoluble, highly cross-linked elastin in NP-untreated cultures were 2.03 ± 0.6 μ g per well, while in case of cells treated with TGF- β 1-releasing NPs, it was about 1.96 ± 0.1 μ g. In the case of alkali-soluble elastic matrix fraction, exogenous TGF- β 1 and NP-released TGF- β 1 attenuated deposition, though in the latter case, soluble elastic matrix amounts were not significantly different from the untreated control cultures. The decrease in soluble-elastin expression/deposition in the exogenous TGF- β 1-treated case is likely due to TGF- β 1 doses being at least 10 fold lower relative to doses previously identified as elastogenic, by our lab (1.0 ng/mL of TGF- β 1) [16, 116]. This lower exogenous dose was delivered here since it matched the amount of TGF- β 1 we determined to be released by NPs. Since TGF- β 1 exhibits biphasic effects, depending on provided dose, it is quite possible that the TGF- β 1 dose delivered in this study (\sim 1 ng/mL over 21 days) to cells did not specifically induce elastogenic effects and contrarily, inhibited elastic matrix production. One interesting observation was that on a per cell basis, total matrix elastin

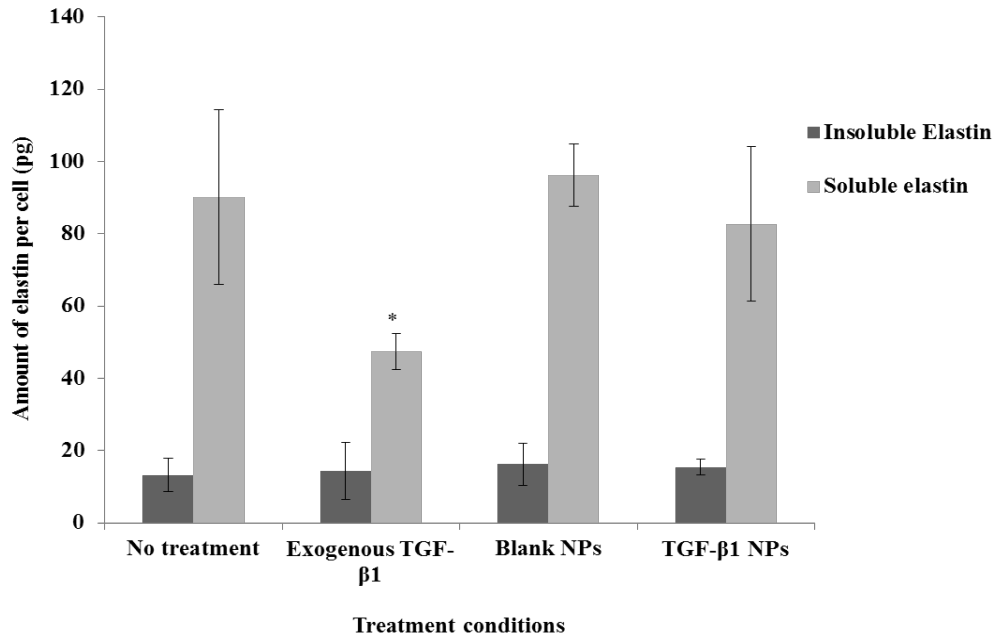


Figure 4.7 Alkali-soluble and –insoluble elastic matrix deposition by EaRASMCs over 21 days of culture, as represented on a per cell basis. Shown results represent mean \pm SD of values obtained by analysis of $n = 6$ cultures/case. * represents significance of difference versus control (no treatment) cultures, deemed for $p < 0.05$.

production was slightly higher in blank NP-treated cultures than in untreated cultures. Although the differences were ultimately deemed statistically not significant, the results suggest that even the blank NPs may have a positive effect on elastic precursor recruitment for crosslinking, which could potentially be attributed to their negative surface charge, which could ‘capture’ and facilitate coacervation/nucleation of the tropoelastin precursors for further cross-linking.

4.7.2 Hydroxy-Proline Assay

The OH-Pro assay estimates the amount of collagen deposits in the ECM of harvested cultures by quantifying amount of OH-Pro residues. The OH-Pro assay on the untreated, exogenous TGF-β1 NPs and treated with blank NPs did not show significant difference to their overall collagen content. However, the cultures treated with NPs loaded with TGF-β1 showed

elevated levels of collagen in their ECM, which were significantly higher ($p \ll 0.01$) compared to the other treatment conditions. Elevated amount of collagen in TGF- β 1-NP treated culture can be attributed to a well-established pro-fibrotic response by EaRASCs, wherein their expression/production of collagen [167, 168] and α -SMA [168] has been documented. The lack of similar effects in cultures supplemented with exogenous TGF- β 1 at concentration equivalent to release achieved from the NPs, and the lack of any effect, positive or negative, with use of blank NPs suggests that a) blank NPs surface modified with PVA do not provide any physical or charge-mediated benefits to collagen precursor capture and/or matrix assembly unlike their effects on elastic matrix assembly, and b) controlled and steady delivery of TGF- β 1 from NPs to cell cultures could provide benefits over delivery of soluble growth factors. The latter aspect

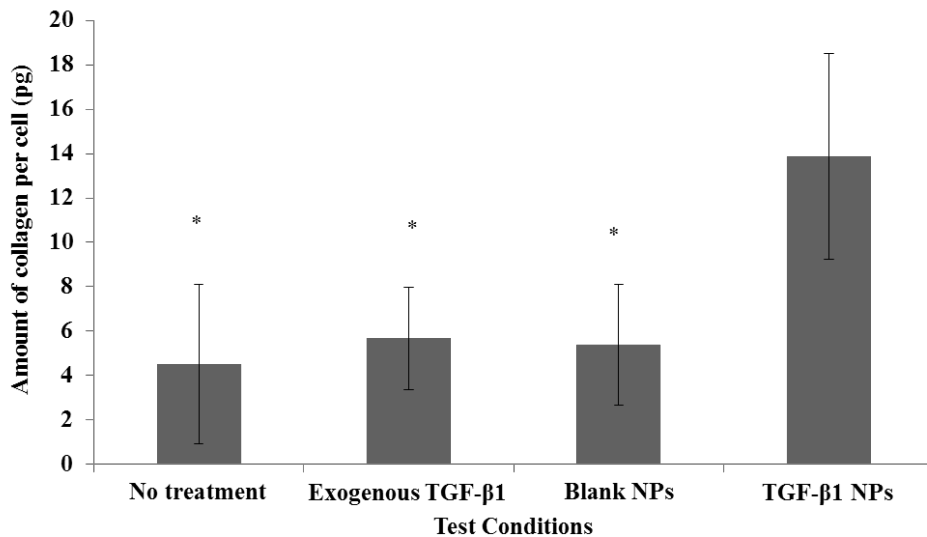


Figure 4.8 Collagen matrix deposition by EaRASCs over 21 days of culture, using the OH-Pro assay and shown on a per cell basis. Shown are the mean \pm SD of amounts determined from assay of $n = 6$ cultures/case. * represents significance of differences versus TGF- β 1 NP-treated cultures, deemed for $p < 0.05$.

could be due to relatively rapid soluble deactivation/loss of activity of exposed, exogenous TGF- β 1 and its transient engagement of all surface receptors as others have suggested with other biomolecular factors [169]. The lack of such effects with NPs may be due to their providing a protective matrix encapsulating TGF- β 1 intactly until it is released.

4.8 Immunofluorescence detection of elastin, fibrillin-1 and LOX

As described in **Section 3.6**, immunofluorescence detection was carried out via confocal microscopy on the paraformaldehyde-fixed, 21-day cell layers, to qualitatively compare deposition of elastin and fibrillin-1, and expression of LOX in cultures that were untreated, or treated with exogenous TGF- β 1, blank NPs, and TGF- β 1-NPs. For this study, three images were taken from different areas in the same culture well. The representative IF images obtained from each of the culture cases are shown in **Figures 4.9, 4.10 and 4.11**, respectively for elastin, fibrillin-1 and LOX.

IF images were obtained from 8 μ m thick cell layer sections. The sections were imaged at 1 μ m thickness intervals and the images were overlaid to create a z-stack composite. These images showed sufficient signal for elastin in all of the treatment conditions. However, cell layers treated with TGF- β 1 exhibited elastic matrix that appeared better organized than control cell layers and those treated with blank NPs. IF images shown in **Figure 4.9** exhibit trends in elastic matrix deposition that mimic trends indicated by the Fastin assay results. Elastin deposition in exogenous TGF- β 1-supplemented cultures appeared to be the least of the four tested cases. Further, in this culture case, most of the elastin appeared to be intracellularly distributed with few visible extracellular structures. As also seen in the results of Fastin assay,

the most intense staining for elastin in the cell layers were in cultures treated with the blank NPs and TGF- β 1-releasing NPs, where the elastin was significantly distributed in the extracellular space and showed greater organization relative to the exogenous TGF- β 1-added cultures and untreated controls.

IF labeling for fibrillin-1 indicated significantly increased expression in cultures treated with TGF- β 1-releasing NPs, compared to any of the other treatments. The expression of fibrillin-1 was localized close to the EaRASMC nuclei especially in control cultures but was far more apparent in the extracellular space for the other treatments, particularly cultures containing TGF- β 1 NPs and exogenous TGF- β 1, in places exhibiting a beads-on-string appearance, which is due to *in vitro* polymerization of fibrillin monomers [170]. These findings are consistent with previously published reports that have shown TGF- β 1 to enhance fibrillin-1 secretion and deposition in cardiac fibroblast cultures [171], and to enhance fibrillin protein synthesis in the ECM of sclerotic skin [172]. Further, previous studies in our own lab have shown TGF- β 1 to upregulate fibrillin-1 deposition and hence elastic fiber formation by vascular SMCs [16]. It was also noted that the cultures/treatments that exhibited the greatest fluorescence due to fibrillin-1 (TGF- β 1 NPs) also exhibited the greatest amounts of elastic matrix deposition, suggesting that enhancing fibrillin deposition will improve elastic matrix assembly.

Previous studies have shown TGF- β 1 to upregulate gene expression synthesis of lysyl oxidase (LOX), a protein/enzyme involved in crosslinking elastin precursors into an alkali-insoluble matrix [173]. Data generated in our lab, have mirrored these findings [16]. In our study, we observed that TGF- β 1, both exogenous and when released from PLGA NPs, significantly enhanced LOX protein synthesis by EaRASMC versus untreated EaRASMC cultures. Despite some increases in LOX protein synthesis by NP-released TGF- β 1 (and

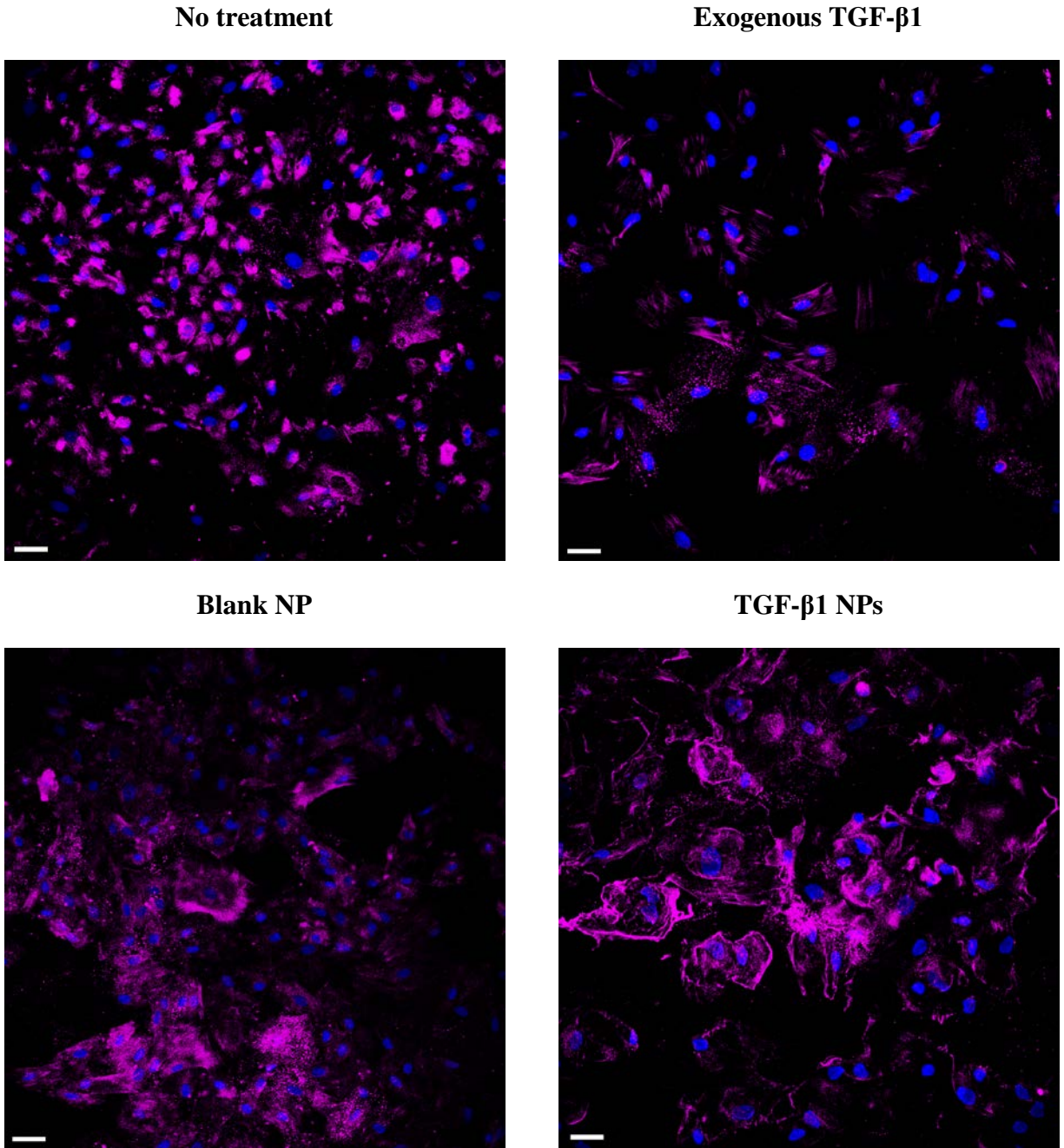


Figure 4.9 Representative images of controls and TGF- β 1 and/or NP-treated EaRASMC cultures IF-labeled for elastin (pink) at 21 days of exposure. DAPI-labeled nuclei appear blue. Magnification: 20 \times . Scale bars represent 50 μ m.

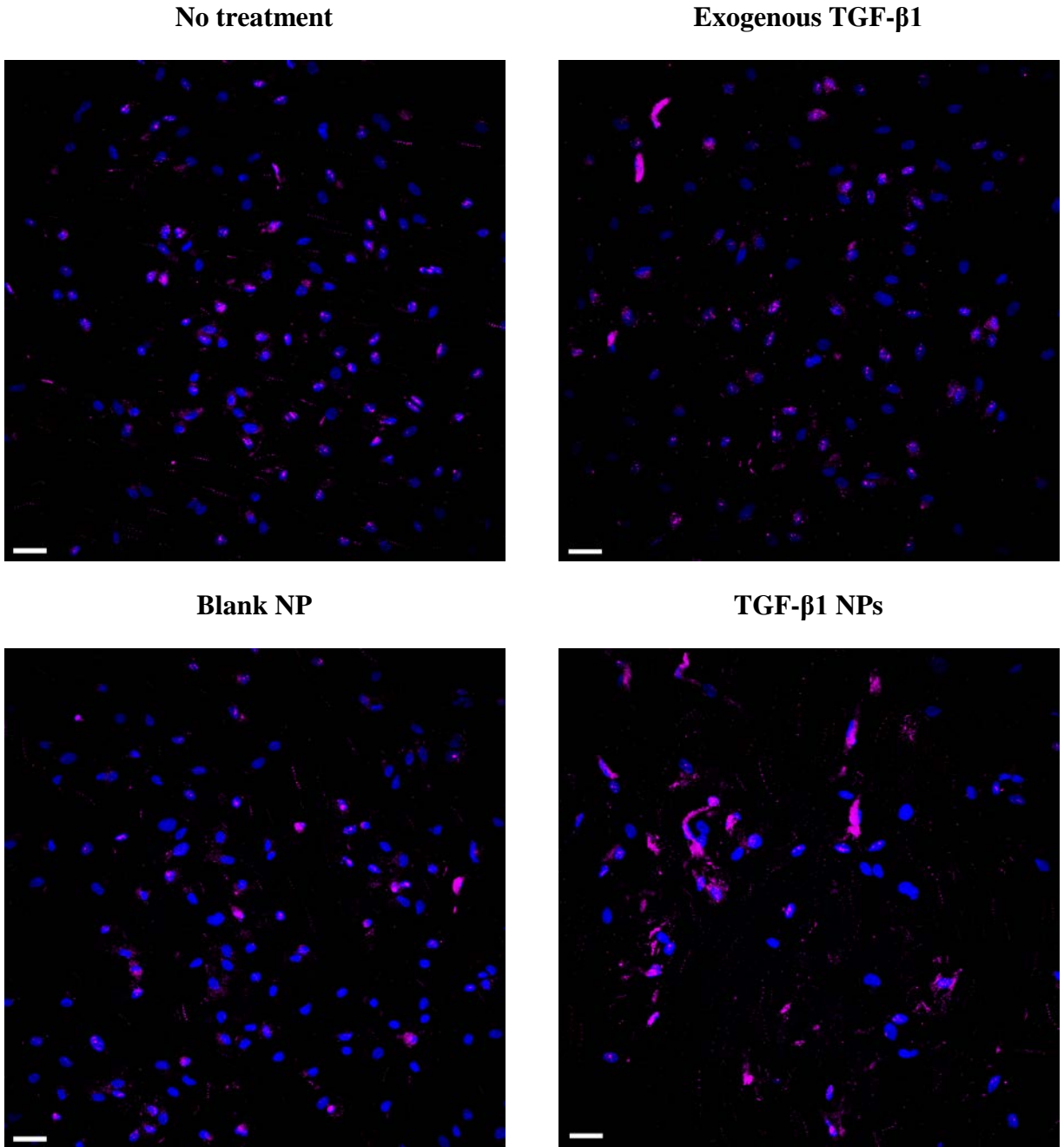


Figure 4.10 Representative images of controls and TGF-β1 and/or NP-treated EaRASC cultures IF-labeled for fibrillin-1 (pink) at 21 days of exposure. DAPI-labeled nuclei appear blue. Magnification: 20×. Scale bars represent 50 μm.

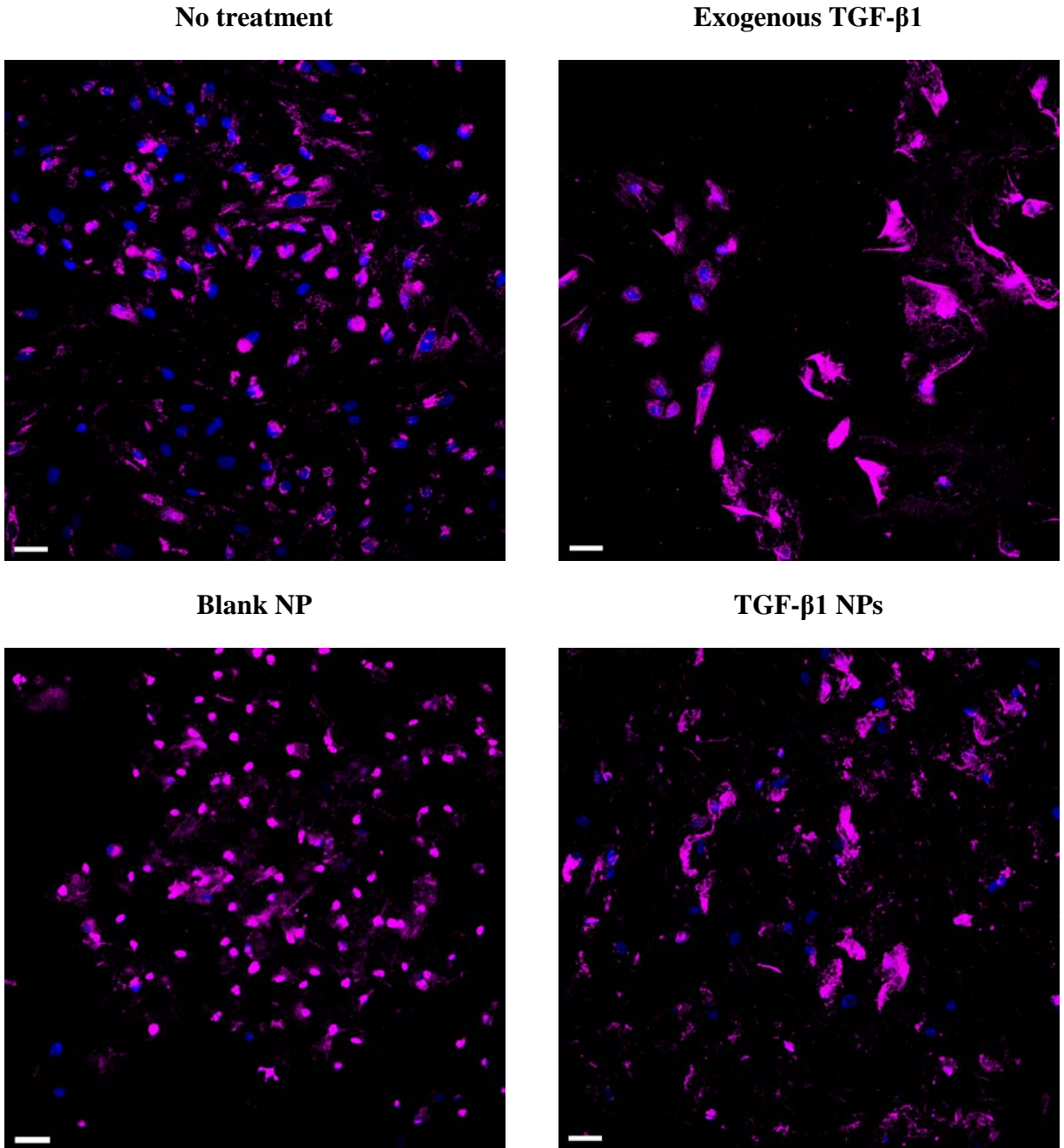


Figure 4.11 Representative images of controls and TGF- β 1 and/or NP-treated EaRASMC cultures IF-labeled for LOX (pink) at 21 days of exposure. DAPI-labeled nuclei appear blue. Magnification: 20 \times . Scale bars represent 50 μ m.

exogenous TGF- β 1), we did not see any dramatic increase in deposited elastic matrix relative to untreated controls. This may be attributed to two factors. The first, mentioned earlier, may be

due to the low delivered doses of TGF- β 1, which were about 1/10th of the elastogenic doses previously identified [16]. The second factor is the inhibiting effect of the negative charge (-27.5 ± 2.2 mV) on the PLGA surface, imparted by the PVA surface modification, on the LOX activity. Studies from the 1970s showed that negatively charged amphiphiles attenuate LOX activity while cationic amphiphiles enhance the same [174]. In separate studies, our lab has shown cationic amphiphiles (e.g., DMAB) used as surfactant for creating PLGA NPs to enhance LOX activity in healthy RASMC cultures. Thus, despite the potential enhancement of LOX protein synthesis by TGF- β 1, the negative surface charge on the NPs may provide a dampening effect (attenuating), resulting lower detection of active LOX protein. On this basis, in future studies, we plan to surface functionalize TGF- β 1 loaded NPs with agents other than DMAB, which impart a positive charge to be able to enhance LOX activity for increased elastin precursor cross-linking and matrix generation.

4.9 Western Blotting for LOX

The results from western blots on cell samples treated with treatment conditions mentioned in **Section 3.7** are illustrated in **Figure 4.12**. The 32 kDa active-LOX protein band was observed to align with the LOX standard in the same gel. We also found substantially bright bands aligning in the molecular weight of \sim 28 kDa, which could be the 28 kDa LOX protein cleavage product [175].

This result suggests the presence of LOX protein qualitatively, and supports the findings of existence of LOX protein deposition visualized in IF studies. The LOX protein bands were quantified using Image J software based on their intensities, and were normalized to band

intensities of β -actin, which served as protein loading controls for each test condition. As illustrated in **Figure 4.13**, we found that cells treated with non-additive treatment deposited the least amount of LOX, based on band intensities. The results were represented as fold change for each test condition, with respect to results obtained in case of untreated controls cultures. Cells treated with exogenous TGF- β 1 produced about 1.9 fold greater LOX, while cells treated with NPs loaded with TGF- β 1 deposited 1.6 fold greater LOX, compared to the non-additive treatment condition.

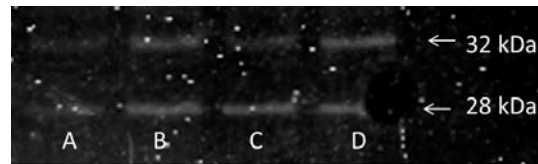


Figure 4.12 Western blot results for LOX (32 kDa - active protein, 28 kDa - cleaved LOX product); lane A contains protein from non-additive treated, lane B contains exogenous TGF- β 1 treated, lane C contains blank NP treated and lane D contains TGF- β 1 NP treated condition.

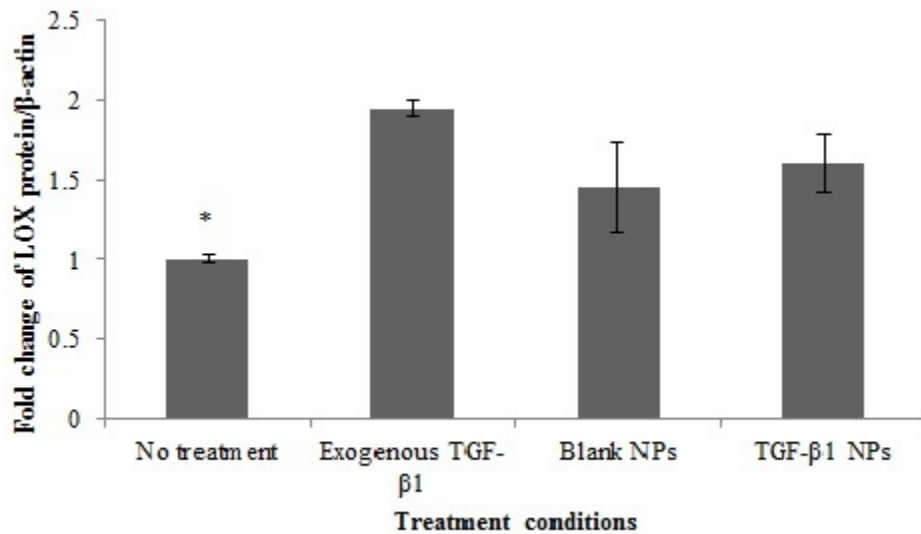


Figure 4.13 Quantification of LOX-protein band intensities, normalized to band intensities of β -actin as visualized in western blots. * represents significant difference ($p < 0.05$) compared to band intensities in TGF- β 1 treated cultures.

4.10 RT-PCR analysis for elastin and elastic matrix assembly proteins

The gene expression of proteins expressed as an effect of treatment of TGF- β 1 released from the NPs was compared to the TGF- β 1-untreated condition, using RT-PCR. The mRNAs served to reverse transcribe the cDNAs and gene expressions of elastin, collagen type-1, fibrillin-1, LOX, and fibulin-5 were examined. The expression of 18S served as inherent control. All the gene expression levels were normalized to that of 18S, and differences in such normalized gene expressions (expressed as relative fluorescence units or RFUs) between controls and TGF- β 1-NP supplemented cultures shown in **Figure 4.14**. The results indicate collagen gene expression to be approximately two times in cultures treated with TGF- β 1 NPs compared to untreated treatment condition, which was statistically significant. These results also align with results of the OH-Pro assay that showed increase in collagen matrix amounts in cultures treated with the TGF- β 1 NPs. The results also indicated LOX up-regulation in TGF- β 1 NP treated cultures reinforcing the semi-quantitative LOX western blot outcomes and the synthesis of LOX observed via IF studies. These results indicate the presence and up-regulation of structural proteins and LOX enzyme which are crucial to the process of synthesizing elastin fibers in ECM of EaRASMCM cultures. However, the TGF- β 1 NP treated cultures exhibited lower levels of mean elastin gene expression, but as described earlier, could be potentially attributable to lower doses of TGF- β 1 released from NPs, compared to dosages previously examined by our lab [16, 116]. The gene expression of fibrillin-1 and fibulin-5 were not deemed as significantly different. Future studies focusing to determine higher TGF- β 1 dosage released from NPs, comparable to exogenous and elastogenic TGF- β 1 dosage identified previously, could potentially generate higher elastin gene expression, significantly different from the controls.

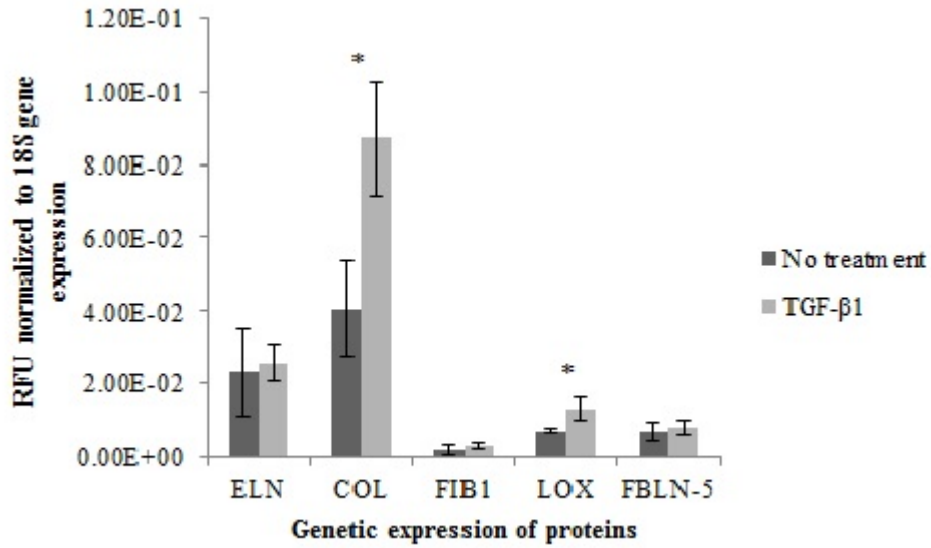


Figure 4.14 Gene expression of proteins of interest represented as RFU from TGF-β1 NP treated and untreated cultures. Shown are the results as mean ± SD of the RFU for different proteins. * represents the gene expression differed significantly between TGF-β1 NP treated and untreated cultures ($p < 0.01$)

CHAPTER V

CONCLUSIONS AND RECOMMENDATIONS

5.1 Conclusions

Our studies demonstrate successful encapsulation of recombinant human TGF- β 1 in PLGA NPs. We were able to generate TGF- β 1 encapsulated NPs exhibiting the desirable average hydrodynamic sizes ranging between 300 to 400 nm, when surface functionalized with both, PVA and DMAB. The TGF- β 1 loaded NPs, surface modified with PVA exhibited high TGF- β 1-entrapment efficiencies, between $74 \pm 15\%$ and $91 \pm 3\%$, depending on TGF- β 1 amounts loaded per mg of NPs. Similarly, the DMAB-NPs too exhibited high TGF- β 1 entrapment efficiencies between 64% and 81%. Muller et. al. have reported that electrostatic repulsions due to surface charge (± 30 mV) result in stable nano-suspensions [134]. Thus, the overall significant negative surface charge (-27.5 mV) of the NPs surface functionalized with PVA, measured as ζ -potential; while positively surface charged TGF- β 1 DMAB-NPs exhibited an average of $+32.2$ mV, both, indicated the stable NP formulation and a deterrent to NP aggregation [176]. Summarizing the properties/characteristics of NPs, our NP formulations showed characteristics deemed desirable in terms of size, charge and encapsulation efficiencies of TGF- β 1.

Our western blot studies confirm that the TGF- β 1 released from PVA-NPs maintains structural integrity, since it generates a protein band that co-localizes with protein bands generated with recombinant TGF- β 1 standards. Additionally, our experiments showed the TGF- β 1 released from PVA-NPs to remain bioactive since it significantly inhibited the proliferation of cultured mink lung epithelial cells (MLCs). We also determined the pattern of release of TGF- β 1 as PLGA NP shell degrades via hydrolysis in PBS system. When PVA-NPs or DMAB-NPs encapsulating TGF- β 1 were suspended in PBS, the TGF- β 1 was released with a high initial burst followed by the 'lag' phase, exhibiting a steady state release of the protein, which was maintained over at least 21 days. However, as described in previous sections, release from DMAB-NPs exhibited artificial ramping up of released TGF- β 1 due to false positive detection of DMAB using ELISA. Future studies will employ alternative detection techniques (e.g., HPLC) to overcome this problem and utilize the positively surface charged NPs on account of their enhanced arterial uptake and affinity to recruit negatively charged LOX.

Even though the TGF- β 1-loaded PVA-NPs released less than 1.0 ng of TGF- β 1 in a 2 day period, a dose we showed previously to be elastogenic, IF images demonstrated higher expression and deposition of elastin in the ECM of EaRSMCs and in a more organized pattern/form in NP- TGF- β 1 treated cultures. Also, they showed higher expression of fibrillin-1, which helps as a scaffolding skeleton for elastin deposition, and LOX, which helps in cross-linking of soluble elastin molecules in TGF- β 1-NP treated cultures when compared to untreated and other control cultures. Semi-quantitative analysis by western blots revealed significantly high amount of LOX presence in NP-TGF- β 1 treated cultures compared to untreated cultures. The amount of collagen deposition in TGF- β 1 NP-treated cultures was also observed to be about 3-fold compared to any other treatment condition, as quantitatively deemed by OH-Pro assay.

These observations were supported by observed upregulated gene expression of collagen, and LOX with respect to untreated cultures, although elastin gene expression was not significantly different from control cultures. The lack of upregulation of elastin gene expression was consistent with lack of increases in elastic matrix deposition in the cultures treated with TGF- β 1-loaded NPs compared to untreated and cultures treated with blank NPs, as demonstrated by Fastin assay. Thus, any improvement in elastic matrix deposition, as gauged using IF, was likely due to improved crosslinking of elastin precursors by LOX, which was seen to be upregulated by TGF- β 1-NPs both at the gene and protein levels.

5.2 Future Recommendations

The continued studies pertaining to elastogenic induction due to TGF- β 1 released from NPs in future will focus on the optimization of several factors from the outcomes of our present study. Few recommendations that can prove fruitful and improve the overall goal of this project are described as follows:

1. Utilize HPLC or other methods to measure release of TGF- β 1 from DMAB-NPs, the positively charged NPs which are more useful from the stand-point of arterial uptake. Additionally, this will enable us to measure fresh TGF- β 1 released at each time point versus frozen aliquots of TGF- β 1, collected over time.
2. Formulate NPs with low molecular weight PLGA or PLGA containing higher glycolide content to accelerate the release of TGF- β 1 towards ultimately achieving higher release over the period of 21 days.
3. Scanning electron microscopy (SEM) of NPs at different time points over 21 days to understand the degradation of PLGA NPs from morphological perspective.

4. Desmosine-isodesmosine assay to assess the level of crosslinking in newly formed elastic matrix of cell cultures.
5. Test other cationic amphiphiles as alternatives to DMAB (e.g., Dodecyltrimethyl ammonium bromide (DTAB), Dodecylamine hydrochloride (DAH)) to impart positive charge to NPs for providing better arterial uptake.
6. Investigate physical implications of NPs: crowding effect on ECM deposition
7. Assess uptake and bio-distribution of NPs in rat aortae, binding to elastic matrix structures, and delivery strategies (i.e., intraluminal infusion with a drug delivery catheter or peri-adventitial injection).
8. Test elastogenic effects if concurrent delivery of HA-o and TGF- β 1 releasing NPs.

REFERENCES

- [1] Reed D, Reed C, Stemmermann G, Hayashi T. Are aortic aneurysms caused by atherosclerosis? *Circulation*. 1992;85:205-11.
- [2] PubMedHealth. Abdominal aortic aneurysm. In: Zieve D, Eltz DR, editors. *ADAM Medical Encyclopedia*: U.S. National Library of Medicine; 2012.
- [3] Maloney JD, Pairolero PC, Smith BF, Hattery RR, Brakke DM, Spittell JA. Ultrasound evaluation of abdominal aortic aneurysms. *Circulation*. 1977;56:80-5.
- [4] Upchurch GR, Schaub TA. Abdominal aortic aneurysm. *Am Fam Physician*. 2006;73:1198-204.
- [5] DeRubertis BG, Trocciola SM, Ryer EJ, Pieracci FM, McKinsey JF, Faries PL, et al. Abdominal aortic aneurysm in women: Prevalence, risk factors, and implications for screening. *J Vasc Surg*. 2007;46:630-5.
- [6] Pyo R, Lee JK, Shipley JM, Curci JA, Mao D, Ziporin SJ, et al. Targeted gene disruption of matrix metalloproteinase-9 (gelatinase B) suppresses development of experimental abdominal aortic aneurysms. *J Clin Invest*. 2000;105:1614-49.
- [7] Wilmink TBM, Quick CRG, Day NE. The association between cigarette smoking and abdominal aortic aneurysms. *J Vasc Surg*. 1999;30:1099-105.
- [8] Greenhalgh RM, Brown LC, Kwong GPS, Powell JT, Thompson SG. Comparison of endovascular aneurysm repair with open repair in patients with abdominal aortic aneurysm (EVAR trial 1), 30-day operative mortality results: randomised controlled trial. *Lancet*. 2004;364:843-8.

- [9] Javerliat I, Di Centa I, Cerceau P, Alfonsi P, Goeau-Brissonniere O, Coggia M. Totally laparoscopic tube graft bypass for infrarenal aortic aneurysm: a well-established surgical technique. *Acta Chirurgica Belgica*. 2006;106:261-6.
- [10] Dake MD, Miller DC, Semba CP, Mitchell RS, Walker PJ, Liddell RP. Transluminal placement of endovascular stent-grafts for the treatment of descending thoracic aortic aneurysms. *N Engl J Med*. 1994;331:1729-34.
- [11] Magennis R, Joekes E, Martin J, White D, McWilliams RG. Complications following endovascular abdominal aortic aneurysm repair. *Br J Radiol*. 2002;75:700-7.
- [12] Hanemaaijer R, Visser H, Koolwijk P, Sorsa T, Salo T, Golub LM, et al. Inhibition of MMP synthesis by doxycycline and chemically modified tetracyclines (CMTs) in human endothelial cells. *Adv Dent Res*. 1998;12:114-8.
- [13] Liu J, Xiong WF, Baca-Regen L, Nagase H, Baxter BT. Mechanism of inhibition of matrix metalloproteinase-2 expression by doxycycline in human aortic smooth muscle cells. *J Vasc Surg*. 2003;38:1376-83.
- [14] Baker AH, Zaltsman AB, George SJ, Newby AC. Divergent effects of tissue inhibitor of metalloproteinase-1, -2, or -3 overexpression on rat vascular smooth muscle cell invasion, proliferation, and death in vitro - TIMP-3 promotes apoptosis. *J Clin Invest*. 1998;101:1478-87.
- [15] Nakashima H, Aoki M, Miyake T, Kawasaki T, Iwai M, Jo N, et al. Inhibition of experimental abdominal aortic aneurysm in the rat by use of decoy oligodeoxynucleotides suppressing activity of nuclear factor kappa B and ets transcription factors. *Circulation*. 2004;109:132-8.

- [16] Kothapalli CR, Taylor PM, Smolenski RT, Yacoub MH, Ramamurthi A. Transforming Growth Factor Beta 1 and Hyaluronan Oligomers Synergistically Enhance Elastin Matrix Regeneration by Vascular Smooth Muscle Cells. *Tissue Engineering Part A*. 2009;15:501-11.
- [17] Kothapalli CR, Ramamurthi A. Benefits of concurrent delivery of hyaluronan and IGF-1 cues to regeneration of crosslinked elastin matrices by adult rat vascular cells. *J Tissue Eng Regen Med*. 2008;2:106-16.
- [18] Shanley CJ, GharaeeKermani M, Sarkar R, Welling TH, Kriegel A, Ford JW, et al. Transforming growth factor-beta(1) increases lysyl oxidase enzyme activity and mRNA in rat aortic smooth muscle cells. *Journal of Vascular Surgery*. 1997;25:446-52.
- [19] Losy F, Dai JP, Pages C, Ginat M, Muscatelli-Groux B, Guinault AM, et al. Paracrine secretion of transforming growth factor-beta(1) in aneurysm healing and stabilization with endovascular smooth muscle cell therapy. *J Vasc Surg*. 2003;37:1301-9.
- [20] Simionescu A, Philips K, Vyavahare N. Elastin-derived peptides and TGF-beta 1 induce osteogenic responses in smooth muscle cells. *Biochem Biophys Res Commun*. 2005;334:524-32.
- [21] Dai JP, Losy F, Guinault AM, Pages C, Anegon I, Desgranges P, et al. Overexpression of transforming growth factor-beta 1 stabilizes already-formed aortic aneurysms - A first approach to induction of functional healing by endovascular gene therapy. *Circulation*. 2005;112:1008-15.
- [22] Danyi P, Elefteriades JA, Jovin IS. Medical Therapy of Thoracic Aortic Aneurysms Are We There Yet? *Circulation*. 2011;124:1469-76.
- [23] Habashi JP, Judge DP, Holm TM, Cohn RD, Loeys BL, Cooper TK, et al. Losartan, an AT1 antagonist, prevents aortic aneurysm in a mouse model of Marfan syndrome. *Science*. 2006;312:117-21.

- [24] Dugdale DC. Artery cut section. In: Zieve D, Eltz DR, editors. ADAM Medical Encyclopedia2012.
- [25] Rasmussen LM, Ledet T. Aortic collagen alterations in human diabetes mellitus. Changes in basement membrane collagen content and in the susceptibility of total collagen to cyanogen bromide solubilisation. *Diabetologia*. 1993;36:445-53.
- [26] Newby AC, Zaltsman AB. Molecular mechanisms in intimal hyperplasia. *J Pathol*. 2000;190:300-9.
- [27] Calver A, Collier J, Vallance P. Nitric-oxide and cardiovascular control. *Exp Physiol*. 1993;78:303-26.
- [28] Edelman ER, Nathan A, Nugent MA. Inhibition of vascular smooth muscle cell proliferation with implanted matrix containing vascular endothelial cells. Massachusetts Institute of Technology; 1998. p. 2788-.
- [29] Schwartz SM, Stemerman MB, Benditt EP. The aortic intima. II. Repair of the aortic lining after mechanical denudation. *Am J Pathol*. 1975;81:15-&.
- [30] Bezie Y, Lacolley P, Laurent S, Gabella G. Connection of smooth muscle cells to elastic lamellae in aorta of spontaneously hypertensive rats. *Hypertension*. 1998;32:166-9.
- [31] Kielty CM, Stephan S, Sherratt MJ, Williamson M, Shuttleworth CA. Applying elastic fibre biology in vascular tissue engineering. *Philos Trans R Soc Lond B Biol Sci*. 2007;362:1293-312.
- [32] Gonzalez MC, Arribas SM, Molero F, Fernandez-Alfonso MS. Effect of removal of adventitia on vascular smooth muscle contraction and relaxation. *Am J Physiol Heart Circ Physiol*. 2001;280:H2876-H81.

- [33] Herman BC, Kundi R, Yamanouchi D, Kent KC, Liu B, Pleshko N. Molecular Analysis of Arterial Remodeling: a Novel Application of Infrared Imaging. In: Farkas DL, Nicolau DV, Leif RC, editors. *Imaging, Manipulation, and Analysis of Biomolecules, Cells, and Tissues* VII 2009.
- [34] Gutterman DD. Adventitia-dependent influences on vascular function. *Am J Physiol Heart Circ Physiol.* 1999;277:H1265-H72.
- [35] Brasselet C, Durand E, Addad F, Zen AAH, Smeets MB, Laurent-Maquin D, et al. Collagen and elastin cross-linking: a mechanism of constrictive remodeling after arterial injury. *Am J Physiol Heart Circ Physiol.* 2005;289:H2228-H33.
- [36] Vorp DA, Schiro BJ, Ehrlich MP, Juvonen TS, Ergin MA, Griffith BP. Effect of aneurysm on the tensile strength and biomechanical behavior of the ascending thoracic aorta. *Ann Thorac Surg.* 2003;75:1210-4.
- [37] Labat Robert J, Szendroi M, Godeau G, Robert L. Comparative distribution patterns of type I and III collagens and fibronectin in human arteriosclerotic aorta. *Pathologie Biologie.* 1985;33:261-5.
- [38] Altman G, Horan R, Martin I, Farhadi J, Stark P, Volloch V, et al. Cell differentiation by mechanical stress. *FASEB J.* 2002;16:270-2.
- [39] Li FY, Redick SD, Erickson HP, Moy VT. Force measurements of the alpha(5)beta(1) integrin-fibronectin interaction. *Biophys J.* 2003;84:1252-62.
- [40] Clark RAF. Fibronectin matrix deposition and fibronectin receptor expression in healing and normal skin. *J Invest Dermatol.* 1990;94:S128-S34.
- [41] Cho J, Mosher DF. Enhancement of thrombogenesis by plasma fibronectin cross-linked to fibrin and assembled in platelet thrombi. *Blood.* 2006;107:3555-63.

- [42] Trial J, Rossen RD, Rubio J, Knowlton AA. Inflammation and Ischemia: Macrophages Activated by Fibronectin Fragments Enhance the Survival of Injured Cardiac Myocytes. *Exp Biol Med.* 2004;229:538-45.
- [43] Hamill KJ, Kligys K, Hopkinson SB, Jones JCR. Laminin deposition in the extracellular matrix: a complex picture emerges. *J Cell Sci.* 2009;122:4409-17.
- [44] Timpl R, Rohde H, Robey PG, Rennard SI, Foidart JM, Martin GR. Laminin - glycoprotein from basement membranes. *J Biol Chem.* 1979;254:9933-7.
- [45] Yanagishita M. Function of proteoglycans in the extracellular matrix. *Acta Pathol Jpn.* 1993;43:283-93.
- [46] Gandhi NS, Mancera RL. The Structure of Glycosaminoglycans and their Interactions with Proteins. *Chem Biol Drug Des.* 2008;72:455-82.
- [47] Jones PA, Scottburden T, Gevers W. Glycoprotein, elastin, and collagen secretion by rat smooth muscle cells. *Proc Natl Acad Sci U S A.* 1979;76:353-7.
- [48] Sephel GC, Davidson JM. Elastin production in human skin fibroblast cultures and its decline with age. *J Invest Dermatol.* 1986;86:279-85.
- [49] Parks WC, Pierce RA, Lee KA, Mecham RP. Elastin1993.
- [50] Scott MJ, Vesely I. Morphology of porcine aortic valve cusp elastin. *J Heart Valve Dis.* 1996;5:464-71.
- [51] Fukuda Y, Ferrans VJ, Crystal RG. Development of elastic fibers of nuchal ligament, aorta, and lung of fetal and postnatal sheep: an ultrastructural and electron microscopic immunohistochemical study. *Am J Anat.* 1984;170:597-629.

- [52] Senior RM, Griffin GL, Mecham RP, Wrenn DS, Prasad KU, Urry DW. Val-Gly-Val-Ala-Pro-Gly, a repeating peptide in elastin, is chemotactic for fibroblasts and monocytes. *J Cell Biol.* 1984;99:870-4.
- [53] Hinek A, Mecham RP, Keeley F, Rabinovitch M. Impaired elastin fiber assembly related to reduced 67-kD elastin-binding protein in fetal lamb ductus arteriosus and in cultured aortic smooth muscle cells treated with chondroitin sulfate. *J Clin Invest.* 1991;88:2083-94.
- [54] Hinek A, Rabinovitch M. 67-kD elastin-binding protein is a protective "companion" of extracellular insoluble elastin and intracellular tropoelastin. *J Cell Biol.* 1994;126:563-74.
- [55] Clarke AW, Wise SG, Cain SA, Kielty CM, Weiss AS. Coacervation is promoted by molecular interactions between the PF2 segment of fibrillin-1 and the domain 4 region of tropoelastin. *Biochemistry.* 2005;44:10271-81.
- [56] Yamauchi Y, Tsuruga E, Nakashima K, Sawa Y, Ishikawa H. Fibulin-4 and -5, but not Fibulin-2, are Associated with Tropoelastin Deposition in Elastin-Producing Cell Culture. *Acta Histochem Cytochem.* 2010;43:131-8.
- [57] Chapman SL, Sicot FX, Davis EC, Huang J, Sasaki T, Chu M-L, et al. Fibulin-2 and Fibulin-5 Cooperatively Function to Form the Internal Elastic Lamina and Protect From Vascular Injury. *Arterioscler Thromb.* 2010;30:68-74.
- [58] Kagan HM, Li WD. Lysyl oxidase: Properties, specificity, and biological roles inside and outside of the cell. *J Cell Biochem.* 2003;88:660-72.
- [59] Sivaraman B, Bashur C, Ramamurthi A. Advances in biomimetic regeneration of elastic matrix structures. *Drug Deliv Transl Res.* 2012;2:323-50.
- [60] Kothapalli CR, Ramamurthi A. Copper nanoparticle cues for biomimetic cellular assembly of crosslinked elastin fibers. *Acta Biomaterialia.* 2009;5:541-53.

- [61] Sherratt MJ. Tissue elasticity and the ageing elastic fibre. *Age*. 2009;31:305-25.
- [62] Johnson DJ, Robson P, Hew Y, Keeley FW. Decreased elastin synthesis in normal development and in long-term aortic organ and cell cultures is related to rapid and selective destabilization of mRNA for elastin. *Circ Res*. 1995;77:1107-13.
- [63] McMahon MP, Faris B, Wolfe BL, Brown KE, Pratt CA, Toselli P, et al. Aging effects on the elastin composition in the extracellular matrix of cultured rat aortic smooth muscle cells. *In Vitro Cell Dev Biol*. 1985;21:674-80.
- [64] Gacchina CE, Deb P, Barth JL, Ramamurthi A. Elastogenic Inductability of Smooth Muscle Cells from a Rat Model of Late Stage Abdominal Aortic Aneurysms. *Tissue Eng Part A*. 2011;17:1699-711.
- [65] Takayama T, Miyata T, Nagawa H. True abdominal aortic aneurysm in Marfan syndrome. *J Vasc Surg*. 2009;49:1162-5.
- [66] Morris CAL, H.M.; Wang,P.P. Williams-Beuren Syndrome: Research, Evaluation, and Treatment: JHU Press; 2006.
- [67] Indik Z, Abrams WR, Kucich U, Gibson CW, Mecham RP, Rosenbloom J. Production of recombinant human tropoelastin: Characterization and demonstration of immunologic and chemotactic activity. *Arch Biochem Biophys*. 1990;280:80-6.
- [68] Grosso LE, Parks WC, Wu L, Mecham RP. Fibroblast adhesion to recombinant tropoelastin expressed as a protein A-fusion protein. *Biochem J*. 1991;273:517-22.
- [69] Faury G, Garnier S, Weiss AS, Wallach J, Fulop T, Jacob MP, et al. Action of tropoelastin and synthetic elastin sequences on vascular tone and on free Ca²⁺ level in human vascular endothelial cells. *Circ Res*. 1998;82:328-36.
- [70] Rodgers UR, Weiss AS. Cellular interactions with elastin. *Pathol Biol*. 2005;53:390-8.

- [71] Perdomo JJ, Gounon P, Schaefferbeke M, Schaefferbeke J, Groult V, Jacob MP, et al. Interaction between cells and elastin fibers: an ultrastructural and immunocytochemical study. *J Cell Physiol.* 1994;158:451-8.
- [72] Thomas EA, Matli JR, Hu JL, Carson MJ, Sutcliffe JG. Pertussis toxin treatment prevents 5-HT5a receptor-mediated inhibition of cyclic AMP accumulation in rat C6 glioma cells. *J Neurosci Res.* 2000;61:75-81.
- [73] Miyamoto K, Atarashi M, Kadozono H, Shibata M, Koyama Y, Okai M, et al. Creation of cross-linked electrospun isotypic-elastin fibers controlled cell-differentiation with new cross-linker. *Int J Biol Macromol.* 2009;45:33-41.
- [74] Brooke BS, Bayes-Genis A, Li DY. New insights into elastin and vascular disease. *Trends Cardiovasc Med.* 2003;13:176-81.
- [75] Thyberg J. Phenotypic: Modulation of smooth muscle cells during formation of neointimal thickenings following vascular injury. *Histol Histopathol.* 1998;13:871-91.
- [76] Larsen M, Artym VV, Green JA, Yamada KM. The matrix reorganized: extracellular matrix remodeling and integrin signaling. *Curr Opin Cell Biol.* 2006;18:463-71.
- [77] Hellmann DB, Grand DJ, Freischlag JA. Inflammatory abdominal aortic aneurysm. *Jama.* 2007;297:395-400.
- [78] Chaikof EL, Brewster DC, Dalman RL, Makaroun MS, Illig KA, Sicard GA, et al. The care of patients with an abdominal aortic aneurysm: The Society for Vascular Surgery practice guidelines. *J Vasc Surg.* 2009;50:2S-49S.
- [79] Daugherty A, Cassis LA. Mouse models of abdominal aortic aneurysms. *Arterioscler Thromb Vasc Biol.* 2004;24:429-34.

- [80] Guo D-C, Papke CL, He R, Milewicz DM. Pathogenesis of thoracic and abdominal aortic aneurysms. In: Tilson MD, Kuivaniemi H, Upchurch GR, editors. *Abdominal Aortic Aneurysm: Genetics, Pathophysiology and Molecular Biology* 2006. p. 339-52.
- [81] Anagnostopoulos PV, Shepard AD, Pipinos, II, Nypaver TJ, Cho JS, Reddy DJ. Factors affecting outcome in proximal abdominal aortic aneurysm repair. *Ann Vasc Surg.* 2001;15:511-9.
- [82] Kazi M, Zhu C, Roy J, Paulsson-Berne G, Hamsten A, Swedenborg J, et al. Difference in Matrix-Degrading Protease Expression and Activity Between Thrombus-Free and Thrombus-Covered Wall of Abdominal Aortic Aneurysm. *Arterioscler Thromb Vasc Biol.* 2005;25:1341-6.
- [83] Defawe OD, Colige A, Lambert CA, Delvenne P, Lapiere CM, Limet R, et al. Gradient of proteolytic enzymes, their inhibitors and matrix proteins expression in a ruptured abdominal aortic aneurysm. *Eur J Clin Invest.* 2004;34:513-4.
- [84] Assar AN. Pharmacological therapy for patients with abdominal aortic aneurysm. *Expert Rev Cardiovasc Ther.* 2009;7:999-1009.
- [85] Rentschler M, Baxter BT. Pharmacological approaches to prevent abdominal aortic aneurysm enlargement and rupture. In: Tilson MD, Kuivaniemi H, Upchurch GR, editors. *Abdominal Aortic Aneurysm: Genetics, Pathophysiology and Molecular Biology* 2006. p. 39-46.
- [86] Sarkar S, Schmitz-Rixen T, Hamilton G, Seifalian AM. Achieving the ideal properties for vascular bypass grafts using a tissue engineered approach: a review. *Med Biol Eng Comput.* 2007;45:327-36.
- [87] Pomar JL. The use of autologous saphenous vein grafts for isolated left anterior descending coronary artery revascularization. *Eur Heart J.* 1995;16:26-8.

- [88] Sodian R, Lueders C, Kraemer L, Kuebler W, Shakibaei M, Reichart B, et al. Tissue engineering of autologous human heart valves using cryopreserved vascular umbilical cord cells. *Ann Thorac Surg.* 2006;81:2207-16.
- [89] Hawkins JA, Breinholt JP, Lambert LM, Fuller TC, Profazer T, McGough EC, et al. Class I and class II anti-HLA antibodies after implantation of cryopreserved allograft material in pediatric patients. *J Thorac Cardiovasc Surg.* 2000;119:324-8.
- [90] Boneva RS, Folks TM. Xenotransplantation and risks of zoonotic infections. *Ann Med.* 2004;36:504-17.
- [91] DiMuzio P, Fischer L, McIlhenny S, DiMatteo C, Golesorhki N, Grabo D, et al. Development of a tissue-engineered bypass graft seeded with stem cells. *Vascular.* 2006;14:338-42.
- [92] Kannan RY, Salacinski HJ, Butler PE, Hamilton G, Seifalian AM. Current status of prosthetic bypass grafts: A review. *J Biomed Mater Res B Appl Biomater.* 2005;74B:570-81.
- [93] Salacinski HJ, Goldner S, Giudiceandrea A, Hamilton G, Seifalian AM, Edwards A, et al. The mechanical behavior of vascular grafts: A review. *J Biomater Appl.* 2001;15:241-78.
- [94] Kim GS, Ahn HJ, Kim WH, Kim MJ, Lee SH. Risk Factors for Postoperative Complications after Open Infrarenal Abdominal Aortic Aneurysm Repair in Koreans. *Yonsei Med J.* 2011;52:339-46.
- [95] Longo GM, Xiong WF, Greiner TC, Zhao Y, Fiotti N, Baxter BT. Matrix metalloproteinases 2 and 9 work in concert to produce aortic aneurysms. *J Clin Invest.* 2002;110:625-32.

- [96] Thompson RW, Baxter BT. MMP inhibition in abdominal aortic aneurysms - Rationale for a prospective randomized clinical trial. In: Greenwald RA, Zucker S, Golub LM, editors. *Inhibition of Matrix Metalloproteinases: Therapeutic Applications* 1999. p. 159-78.
- [97] Ding R, McGuinness CL, Burnand KG, Sullivan E, Smith A. Matrix Metalloproteinases in the Aneurysm Wall of Patients Treated with Low-Dose Doxycycline. *Vascular*. 2005;13:290-7.
- [98] Baxter BT, Pearce WH, Waltke EA, Littooy FN, Hallett JW, Kent KC, et al. Prolonged administration of doxycycline in patients with small asymptomatic abdominal aortic aneurysms: Report of a prospective (Phase II) multicenter study. *J Vasc Surg*. 2002;36:1-12.
- [99] Chang WYC, Clements D, Johnson SR. Effect of doxycycline on proliferation, MMP production, and adhesion in LAM-related cells. *Am J Physiol Lung Cell Mol Physiol*. 2010;299:L393-L400.
- [100] Franco C, Ho B, Mulholland D, Hou GP, Islam M, Donaldson K, et al. Doxycycline alters vascular smooth muscle cell adhesion, migration, and reorganization of fibrillar collagen matrices. *Am J Pathol*. 2006;168:1697-709.
- [101] Waugh JM, Li-Hawkins J, Yuksel E, Cifra PN, Amabile PG, Hilfiker PR, et al. Therapeutic elastase inhibition by alpha-1-antitrypsin gene transfer limits neointima formation in normal rabbits. *J Vasc Interv Radiol*. 2001;12:1203-9.
- [102] Lemarchand P, Jaffe HA, Danel C, Cid MC, Kleinman HK, Stratfordperricaudet LD, et al. Adenovirus-mediated transfer of a recombinant human alpha 1-antitrypsin cDNA to human endothelial cells. *Proc Natl Acad Sci U S A*. 1992;89:6482-6.
- [103] Isenburg JC, Simionescu DT, Starcher BC, Vyavahare NR. Elastin stabilization for treatment of abdominal aortic aneurysms. *Circulation*. 2007;115:1729-37.

- [104] Greenwood HL, Thorsteinsdottir H, Perry G, Renihan J, Singer PA, Daar AS. Regenerative medicine: new opportunities for developing countries. *Int J Biotechnol.* 2006;8:60-77.
- [105] Mason C, Dunnill P. A brief definition of regenerative medicine. *Regen Med.* 2008;3:1-5.
- [106] Kneser U, Schaefer DJ, Polykandriotis E, Horch RE. Tissue engineering of bone: the reconstructive surgeon's point of view. *J Cell Mol Med.* 2006;10:7-19.
- [107] Mecham RP, Levy BD, Morris SL, Madaras JG, Wrenn DS. Increased cyclic GMP levels lead to a stimulation of elastin production in ligament fibroblasts that is reversed by cyclic AMP. *J Biol Chem.* 1985;260:3255-8.
- [108] Mecham RP, Lange G, Madaras J, Starcher B. Elastin synthesis by ligamentum nuchae fibroblasts: effects of culture conditions and extracellular matrix on elastin production. *J Cell Biol.* 1981;90:332-8.
- [109] Rich CB, Goud HD, Bashir M, Rosenbloom J, Foster JA. Developmental regulation of aortic elastin gene expression involves disruption of an IGF-I sensitive repressor complex. *Biochem Biophys Res Commun.* 1993;196:1316-22.
- [110] Davidson JM, LuValle PA, Zoia O, Quaglino D, Giro MG. Ascorbate differentially regulates elastin and collagen biosynthesis in vascular smooth muscle cells and skin fibroblasts by pretranslational mechanisms. *J Biol Chem.* 1997;272:345-52.
- [111] Barone LM, Faris B, Chipman SD, Toselli P, Oakes BW, Franzblau C. Alteration of the extracellular matrix of smooth muscle cells by ascorbate treatment. *Biochimica Et Biophysica Acta.* 1985;840:245-54.
- [112] Brettell LM, McGowan SE. Basic fibroblast growth factor decreases elastin production by neonatal rat lung fibroblasts. *Am J Respir Cell Mol Biol.* 1994;10:306-15.

- [113] Davis EC, Mecham RP. Intracellular trafficking of tropoelastin. *Matrix Biol.* 1998;17:245-54.
- [114] Frisch SM, Davidson JM, Werb Z. Blockage of tropoelastin secretion by monensin represses tropoelastin synthesis at a pretranslational level in rat smooth muscle cells. *Mol Cell Biol.* 1985;5:253-8.
- [115] Wolfe BL, Rich CB, Goud HD, Terpstra AJ, Bashir M, Rosenbloom J, et al. Insulin-like growth factor-I regulates transcription of the elastin gene. *J Biol Chem.* 1993;268:12418-26.
- [116] Kothapalli CR, Gacchina CE, Ramamurthi A. Utility of Hyaluronan Oligomers and Transforming Growth Factor-Beta1 Factors for Elastic Matrix Regeneration by Aneurysmal Rat Aortic Smooth Muscle Cells. *Tissue Engineering Part A.* 2009;15:3247-60.
- [117] Joddar B, Ramamurthi A. Fragment size- and dose-specific effects of hyaluronan on matrix synthesis by vascular smooth muscle cells. *Biomaterials.* 2006;27:2994-3004.
- [118] Joddar B, Ramamurthi A. Elastogenic effects of exogenous hyaluronan oligosaccharides on vascular smooth muscle cells. *Biomaterials.* 2006;27:5698-707.
- [119] Mitts TF, Bunda S, Wang YT, Hinek A. Aldosterone and Mineralocorticoid Receptor Antagonists Modulate Elastin and Collagen Deposition in Human Skin. *J Invest Dermatol.* 2010;130:2396-406.
- [120] Hayashi A, Suzuki T, Tajima S. MODULATIONS OF ELASTIN EXPRESSION AND CELL-PROLIFERATION BY RETINOIDS IN CULTURED VASCULAR SMOOTH-MUSCLE CELLS. *Journal of Biochemistry.* 1995;117:132-6.
- [121] Tajima S, Hayashi A, Suzuki T. Elastin expression is up-regulated by retinoic acid but not by retinol in chick embryonic skin fibroblasts. *Journal of Dermatological Science.* 1997;15:166-72.

- [122] Kothapalli CR, Ramamurthi A. Lysyl oxidase enhances elastin synthesis and matrix formation by vascular smooth muscle cells. *Journal of Tissue Engineering and Regenerative Medicine*. 2009;3:655-61.
- [123] Joddar B, Ibrahim S, Ramamurthi A. Impact of delivery mode of hyaluronan oligomers on elastogenic responses of adult vascular smooth muscle cells. *Biomaterials*. 2007;28:3918-27.
- [124] Hirano S, Bless DM, Heisey D, Ford CN. Effect of growth factors on hyaluronan production by canine vocal fold fibroblasts. *Annals of Otology Rhinology and Laryngology*. 2003;112:617-24.
- [125] Brettell LM, McGowan SE. Basic fibroblast growth factor decreases elastin production by neonatal rat lung fibroblasts. *Am J Respir Cell Mol Biol*. 1994;10:306-15.
- [126] Rodriguez C, Rodriguez-Sinovas A, Martinez-Gonzalez J. Lysyl oxidase as a potential therapeutic target. *Drug News Perspect*. 2008;21:218-24.
- [127] Smith-Mungo LI, Kagan HM. Lysyl oxidase: Properties, regulation and multiple functions in biology. *Matrix Biology*. 1998;16:387-98.
- [128] Davidson JM, Zoia O, Liu JM. Modulation of transforming growth factor-beta 1 stimulated elastin and collagen production and proliferation in porcine vascular smooth muscle cells and skin fibroblasts by basic fibroblast growth factor, transforming growth factor-alpha, and insulin-like growth factor-I. *J Cell Physiol*. 1993;155:149-56.
- [129] Yamamoto M, Aoyagi M, Tajima S, Wachi H, Fukai N, Matsushima Y, et al. Increase in elastin gene expression and protein synthesis in arterial smooth muscle cells derived from patients with moyamoya disease. *Stroke*. 1997;28:1733-8.
- [130] Marigo V, Volpin D, Vitale G, Bressan GM. Identification of a TGF-beta responsive element in the human elastin promoter. *Biochem Biophys Res Commun*. 1994;199:1049-56.

- [131] Bala I, Hariharan S, Kumar M. PLGA nanoparticles in drug delivery: The state of the art. *Crit Rev Ther Drug Carrier Syst.* 2004;21:387-422.
- [132] Panyam J, Labhasetwar V. Biodegradable nanoparticles for drug and gene delivery to cells and tissue. *Adv Drug Deliv Rev.* 2003;55:329-47.
- [133] Kwon HY, Lee JY, Choi SW, Jang YS, Kim JH. Preparation of PLGA nanoparticles containing estrogen by emulsification-diffusion method. *Colloids and Surfaces a-Physicochemical and Engineering Aspects.* 2001;182:123-30.
- [134] Muller RH, Jacobs C, Kayser O. Nanosuspensions as particulate drug formulations in therapy Rationale for development and what we can expect for the future. *Adv Drug Deliv Rev.* 2001;47:3-19.
- [135] Song CX, Labhasetwar V, Cui XM, Underwood T, Levy RJ. Arterial uptake of biodegradable nanoparticles for intravascular local drug delivery: Results with an acute dog model. *J Control Release.* 1998;54:201-11.
- [136] Makadia HK, Siegel SJ. Poly Lactic-co-Glycolic Acid (PLGA) as Biodegradable Controlled Drug Delivery Carrier. *Polymers.* 2011;3:1377-97.
- [137] Kobsa S, Saltzman WM. Bioengineering approaches to controlled protein delivery. *Pediatr Res.* 2008;63:513-9.
- [138] Busch W, Bastian S, Trahorsch U, Iwe M, Kuhnel D, Meissner T, et al. Internalisation of engineered nanoparticles into mammalian cells in vitro: influence of cell type and particle properties. *J Nanopart Res.* 2011;13:293-310.
- [139] Harkin DW, Romaschin A, Taylor SM, Rubin BB, Lindsay TF. Complement C5a receptor antagonist attenuates multiple organ injury in a model of ruptured abdominal aortic aneurysm. *J Vasc Surg.* 2004;39:196-206.

- [140] Lu L, Peter SJ, Lyman MD, Lai HL, Leite SM, Tamada JA, et al. In vitro and in vivo degradation of porous poly(DL-lactic-co-glycolic acid) foams. *Biomaterials*. 2000;21:1837-45.
- [141] Park TG. Degradation of poly(lactic-co-glycolic acid) microspheres: effect of copolymer composition. *J Control Release*. 1994;30:161-73.
- [142] De Jong WH, Borm PJA. Drug delivery and nanoparticles: Applications and hazards. *Int J Nanomedicine*. 2008;3:133-49.
- [143] Anderson JM, Shive MS. Biodegradation and biocompatibility of PLA and PLGA microspheres. *Adv Drug Deliv Rev*. 1997;28:5-24.
- [144] Lu LC, Yaszemski MJ, Mikos AG. TGF-beta 1 release from biodegradable polymer microparticles: Its effects on marrow stromal osteoblast function. *J Bone Joint Surg Am*. 2001;83A:S82-S91.
- [145] Astete CE, Sabliov CM. Synthesis and characterization of PLGA nanoparticles. *J Biomater Sci Polym Ed*. 2006;17:247-89.
- [146] Xu A, Yao M, Xu G, Ying J, Ma W, Li B, et al. A physical model for the size-dependent cellular uptake of nanoparticles modified with cationic surfactants. *Int J Nanomedicine*. 2012;7:3547-54.
- [147] Kagan HM, Simpson DE, Tseng L. Substrate-directed modulation of elastin oxidation by lysyl oxidase. *Connect Tissue Res*. 1981;8:213-7.
- [148] Kagan HM, Tseng L, Simpson DE. Control of elastin metabolism by elastin ligands. Reciprocal effects on lysyl oxidase activity. *J Biol Chem*. 1981;256:5417-21.
- [149] Davda J, Labhasetwar V. Sustained Proangiogenic Activity of Vascular Endothelial Growth Factor Following Encapsulation in Nanoparticles. *Journal of Biomedical Nanotechnology*. 2005;1:74-82.

- [150] Howe PH, Cunningham MR, Leof EB. Inhibition of mink lung epithelial cell proliferation by transforming growth factor-beta is coupled through a pertussis-toxin-sensitive substrate. *Biochem J.* 1990;266:537-43.
- [151] Helpern VJ, Nackman GB, Gandhi RH, Irizarry E, Scholes JV, Ramey WG, et al. The elastase infusion model of experimental aortic aneurysms: synchrony of induction of endogenous proteinases with matrix destruction and inflammatory cell response. *J Vasc Surg.* 1994;20:51-60.
- [152] Labarca C, Paigen K. A simple, rapid, and sensitive DNA assay procedure. *Analytical Biochemistry.* 1980;102:344-52.
- [153] Reddy GK, Enwemeka CS. A simplified method for the analysis of hydroxyproline in biological tissues. *Clin Biochem.* 1996;29:225-9.
- [154] Risteli J, Tuderman L, Kivirikko KI. Intracellular enzymes of collagen biosynthesis in rat liver as a function of age and in hepatic injury induced by dimethylnitrosamine. Purification of rat prolyl hydroxylase and comparison of changes in prolyl hydroxylase activity with changes in immunoreactive prolyl hydroxylase. *Biochem J.* 1976;158:369-76.
- [155] Bashur CA, Shaffer RD, Dahlgren LA, Guelcher SA, Goldstein AS. Effect of Fiber Diameter and Alignment of Electrospun Polyurethane Meshes on Mesenchymal Progenitor Cells. *Tissue Engineering Part A.* 2009;15:2435-45.
- [156] Rutledge RG, Stewart D. A kinetic-based sigmoidal model for the polymerase chain reaction and its application to high-capacity absolute quantitative real-time PCR. *Bmc Biotechnol.* 2008;8.
- [157] Leigh DR, Mesiha M, Baker AR, Walker E, Derwin KA. Host response to xenograft ECM implantation is not different between the shoulder and body wall sites in the rat model. *J Orthop Res.* 2012;30:1725-31.

- [158] Panyam J, Dali MA, Sahoo SK, Ma WX, Chakravarthi SS, Amidon GL, et al. Polymer degradation and in vitro release of a model protein from poly(D,L-lactide-co-glycolide) nano- and microparticles. *J Control Release*. 2003;92:173-87.
- [159] Murakami H, Kobayashi M, Takeuchi H, Kawashima Y. Utilization of poly(DL-lactide-co-glycolide) nanoparticles for preparation of mini-depot tablets by direct compression. *J Control Release*. 2000;67:29-36.
- [160] Davda J, Labhasetwar V. Sustained Proangiogenic Activity of Vascular Endothelial Growth Factor Following Encapsulation in Nanoparticles. *J Biomed Nanotechnol*. 2005;1:74-82.
- [161] Labhasetwar V, Song CX, Humphrey W, Shebuski R, Levy RJ. Arterial uptake of biodegradable nanoparticles: Effect of surface modifications. *J Pharm Sci*. 1998;87:1229-34.
- [162] Lu L, Stamatias GN, Mikos AG. Controlled release of transforming growth factor beta 1 from biodegradable polymer microparticles. *J Biomed Mater Res*. 2000;50:440-51.
- [163] Jhunjhunwala S, Balmert SC, Raimondi G, Dons E, Nichols EE, Thomson AW, et al. Controlled release formulations of IL-2, TGF-beta 1 and rapamycin for the induction of regulatory T cells. *J Control Release*. 2012;159:78-84.
- [164] Jennings V, Thunemann AF, Gohla SH. Characterisation of a novel solid lipid nanoparticle carrier system based on binary mixtures of liquid and solid lipids. *Int J Pharm*. 2000;199:167-77.
- [165] Sivaraman BRA. Multifunctional Nanoparticles for Doxycycline Delivery towards Localized Elastic Matrix Stabilization and Regenerative Repair. *Biomaterials*. 2012.
- [166] Sakakibara K, Kubota K, Worku B, Hollenbeck S, Faries P, Liu B, et al. TGF-beta inhibits vascular smooth muscle cell proliferation through down regulation of cyclin A. *J Surg Res*. 2003;114:283.

- [167] Roberts AB, Sporn MB, Assoian RK, Smith JM, Roche NS, Wakefield LM, et al. Transforming growth factor type beta: rapid induction of fibrosis and angiogenesis in vivo and stimulation of collagen formation in vitro. *Proc Natl Acad Sci U S A*. 1986;83:4167-71.
- [168] Leask A, Abraham DJ. TGF-beta signaling and the fibrotic response. *FASEB J*. 2004;18:816-27.
- [169] Deed R, Rooney P, Kumar P, Norton JD, Smith J, Freemont AJ, et al. Early-response gene signalling is induced by angiogenic oligosaccharides of hyaluronan in endothelial cells. Inhibition by non-angiogenic, high-molecular-weight hyaluronan. *Int J Canc Prev*. 1997;71:251-6.
- [170] Dietz HC, Pyeritz RE. Mutations in the human gene for fibrillin-1 (FBN1) in the Marfan syndrome and related disorders. *Hum Mol Genet*. 1995;4:1799-809.
- [171] Bouzeghrane F, Reinhardt DP, Reudelhuber TL, Thibault G. Enhanced expression of fibrillin-1, a constituent of the myocardial extracellular matrix in fibrosis. *Am J Physiol Heart Circ Physiol*. 2005;289:H982-H91.
- [172] Kissin EY, Lemaire R, Korn JH, Lafyatis R. Transforming growth factor beta induces fibroblast fibrillin-1 matrix formation. *Arthritis Rheum*. 2002;46:3000-9.
- [173] Sethi A, Mao WM, Wordinger RJ, Clark AF. Transforming Growth Factor-beta Induces Extracellular Matrix Protein Cross-Linking Lysyl Oxidase (LOX) Genes in Human Trabecular Meshwork Cells. *Invest Ophthalmol Vis Sci*. 2011;52:5240-50.
- [174] Trackman PC, Olsson TA, Sullivan KA, Kagan HM. Purification and inhibitors of bovine aortic lysyl oxidase. *Fed Proc*. 1978;37:1530-.

[175] Sommer P, Gleyzal C, Raccurt M, Delbourg M, Serrar M, Joazeiro P, et al. Transient expression of lysyl oxidase by liver myofibroblasts in murine schistosomiasis. *Lab Invest.* 1993;69:460-70.

[176] Hans ML, Lowman AM. Biodegradable nanoparticles for drug delivery and targeting. *Curr Opin Solid State Mater Sci.* 2002;6:319-27.